THE THERMODYNAMIC PROPERTIES OF THE OXIDE SYSTEMS CaO-MgO-SiO_2 AND MgO-Al_2O_3-SiO_2

by

D. HENDERSON, B.Sc., A.R.C.S.T.

Thesis submitted to the University of Glasgow
for the degree of Doctor of Philosophy

January, 1964

ProQuest LLC.
789 East Eisenhower Parkway
P.O. Box 1346
Ann Arbor, MI 48106 – 1346

THE THERMODYNAMIC PROPERTIES OF THE OXIDE SYSTEMS

$CaO-MgO-SiO_2$ and $MgO-Al_2O_3-SiO_2$

SUMMARY

The slags used in metallurgical processes are usually very complex in nature, being ternary, quaternary, and even more complex. Complete investigation of the thermodynamic properties of even a portion of such a complex system would involve a very large amount of work even if all the experimental difficulties were solved. Secondly, it is difficult to interpret measurements made on complex slags without first knowing and understanding how simple binary and ternary melts behave.

For these reasons, investigators decided to build up thermodynamic data on the simpler binary and ternary melts in the hope that an examination of these data might lead to "models" by which the knowledge of the simpler systems could be used to predict the thermodynamic properties of the more complex slags used in industrial processes.

Variation in the thermodynamic activity with composition has been examined in a number of binary and ternary systems and "models" have been suggested by Richardson, Flood et al, and

Lumsden. Further experimental work is required and in the present work, the activities of silica in the ternary oxide systems CaO-MgO-SiO_2 and MgO-Al_2O_3-SiO_2 have been determined by placing a compact containing pure silica, graphite and silicon carbide in a graphite crucible and allowing it to come to equilibrium with carbon monoxide at 1500°C and 1550°C as represented by the following equation

$$SiO_2\ (\beta\ \mathrm{crist}) + 3C(\mathrm{gr}) = SiC(\mathrm{cub.}) + 2CO(g) \ldots\ldots\ldots (1)$$

The reaction must be considered as the summation of two other reactions

$$SiO_2\ (\beta\ \mathrm{crist}) + C(\mathrm{gr}) = SiO(g) + Co(g) \ldots\ldots\ldots\ldots (2)$$

$$SiO\ (g) + 2C\ (\mathrm{gr}) = SiC(\mathrm{cub.}) + CO(g) \ldots\ldots\ldots (3)$$

The equilibrium pressure ($pCO + pSiO$) was measured at 1500°C and 1550°C. Silica, graphite and silicon carbide were all in their standard states therefore the equilibrium constant for reaction (1), $K_1 = p^2 CO(\mathrm{standard})$. The partial pressure of CO in the system was obtained from the measured reaction pressure ($pCO + pSiO$) and the equilibrium constant for reaction (2) $K_2 = p\ SiO.\ p\ CO$. Substitution of a compact containing the slag yields values of p CO (slag), this being obtained from the measured equilibrium pressure (p CO + p SiO) and the equilibrium constant for reaction (3), $K_3 = \frac{pCO}{pSiO}$. The silica activity of the slag, referred to the standard state of β cristobalite, is given by p^2 CO(slag)/p^2 CO (standard). In the CaO-MgO-SiO_2 system silica activities were obtained along lines of constant magnesia content, i.e. 10, 20 and 30% magnesia, at both 1500°C and 1550°C. The activities of the other two components were calculated using Schumann's application of the Gibbs-Duhem equation. The results obtained in the CaO-MgO-SiO_2 system were compared with data obtained by Rein and Chipman and also Sawamura. The results were examined with regard to Richardson's model and it has been shown that this model does not hold in the CaO-MgO-SiO_2 system. Values have been obtained for the free energies of formation of the interoxide compounds in this system from the present results and are compared with those given by Kelley.

In the MgO-Al_2O_3-SiO_2 system silica activities were obtained along lines of constant alumina content, i.e. 10, 20 and 30% alumina, at both 1500°C and 1550°C. The activities of the other two components were calculated using Schumann's application of the Gibbs-Duhem equation. The results obtained in the MgO-Al_2O_3-SiO_2 system were compared with data obtained by Rein and

Chipman. The present results have also been used to obtain values for the free energy of formation of the interoxide compounds in this system.

CONTENTS

CHAPTER I

INTRODUCTION

INTRODUCTION

The slags used in metallurgical processes are usually very complex in nature, being ternary, quaternary, and even more complex. For example, in steel-making processes the oxides which form the major part of the slags encountered are FeO, CaO, MnO and SiO_2 but smaller amounts of MgO, Al_2O_3 and P_2O_5 can be present. Complete investigation of the thermodynamic properties of even a portion of such a complex system would involve a very large amount of work even if all the experimental difficulties were solved. Secondly, it is difficult to interpret measurements made on complex slags without first knowing and understanding how simple binary and ternary melts behave.

For these reasons, investigators who were interested in the thermodynamic properties of slag solutions decided to build up thermodynamic data on the simpler binary and ternary melts in the hope that an examination of these data might lead to 'models' by which the knowledge of the simpler systems could be used to predict the thermodynamic properties of the more complex slags used in industrial processes.

Variation in the thermodynamic activity with composition has been examined in the binary system $CaO-SiO_2$ by a number of investigators [1, 2, 3, 4, 5, 6, 7]. The earlier work [1, 2, 3] gave data which were contradictory but the later investigations show good agreement at 1500°C between the data of Sharma and Richardson [4] and those of Kay and Taylor [5] for mole fractions of silica greater than 0·5. Extrapolation of both these data to 1630°C gives fairly good agreement with Sanbongi and Omori [6]. At silica mole fractions less than 0·5 (as the calcium orthosilicate saturation surface is closely approached) the data of Sanbongi and Omori and of Sharma and Richardson give lower activities than Kay and Taylor when compared at the same temperature. Data obtained by Chipman [7] when recalculated using recent free energy data for silica and silicon in iron give lower activities than Kay and Taylor in this range. Thus the activities in the binary system $CaO-SiO_2$ are well established for mole fractions of silica greater than 0·5.

Other binaries in which activities are well established are the systems $FeO-SiO_2$ [8, 9], $MnO-SiO_2$ [10] and $PbO-SiO_2$ [11]. The lime activities at 1500°C in the $CaO-Al_2O_3$ system have been estimated by both Sharma and Richardson [4] and Carter and MacFarlane [3] from studies of sulphur distribution. Chipman [7] also estimated the lime activities by combining free-energy data with Carter and MacFarlane's Cs values. The agreement between the three sets of results is poor although it improves at the higher lime concentrations.

The first investigation of activities in a ternary melt was carried out by Chipman and co-workers [12, 13] in which the activities of ferrous oxide were determined in the ternary system FeO-CaO-SiO_2 at 1600°C. The melts investigated also contained small amounts of MgO and MnO and from the data obtained, it appeared that the three basic oxides, CaO, MgO and MnO, were equivalent in their effect on the ferrous oxide activities. A later investigation [14] showed that this was not the case and that replacement of CaO by MgO raises the ferrous oxide activity. Activities of ferrous oxide have also been determined by Bodsworth [9] in the system CaO-FeO-SiO_2 in the temperature range 1265 - 1365°C. Extrapolation of these data to 1600°C gives good agreement with the previous data up to 20 mole per cent of lime but at higher lime contents the extrapolated data give lower ferrous oxide activities.

Richardson and co-workers [15, 16] have investigated the ternaries CaO-PbO-SiO_2, MgO-PbO-SiO_2, PbO-ZnO-SiO_2 and CaO-MnO-SiO_2 and have found that the pattern of activities found in the system CaO-FeO-SiO_2 is broadly followed in these systems.

Other systems which have been investigated are the ternaries FeO-SiO_2-Fe_2O_3 [17], FeO-MnO-SiO_2 [18], MnO-CaO-SiO_2 [10] and CaO-Al_2O_3-SiO_2 [5]. In some of these investigations measurements were also made on more complex melts.

As mentioned previously, the ternary systems $CaO-FeO-SiO_2$, $CaO-MnO-SiO_2$ and $CaO-PbO-SiO_2$ show a similar pattern of iso-activity lines and Richardson has examined these lines with a view to obtaining a model which would explain them. The heats of formation for solid solutions of binary silicates of equal silica mole fraction, such as $CaO.SiO_2$ + $FeO.SiO_2$ and $2FeO.SiO_2$ + $2MgO.SiO_2$, are very small and can be considered to be within experimental error. Richardson is of the opinion that these binary silicates mix ideally in the solid state, i.e. there is no heat of mixing, no change in the anionic structure from one binary to the other and thus the free energy of mixing arises only from the random mixing of the cations with each other. If it is assumed that ideal mixing takes place in the liquid as well as the solid state then it is possible to calculate activities in the ternaries from the activities in the appropriate binaries [16]. If this is done it appears that this model holds in the systems $FeO-CaO-SiO_2$ [10], $MnO-CaO-SiO_2$ [19] and $FeO-MnO-SiO_2$ [20] down to about the metasilicate composition. In the more basic melts there are negative free energies of mixing of 1 to 2 k cal/mole oxide.

Flood and co-workers [21, 22] have attempted to calculate activities in highly basic melts from ionic theory. Like Richardson, they assume random mixing of the cations but they consider that the free energy of mixing arises from both the entropy of mixing and changes that take place in the cation-anion bonds. For example, when ferrous oxide and calcium orthosilicate are mixed to form liquid solution, $Fe^{2+}\,SiO_4^{4-}$ and $Ca^{2+}\,O^{2-}$ bonds are formed, while some $Ca^{2+}\,SiO_4^{4-}$ and $Fe^{2+}\,O^{2-}$ bonds are broken. From such considerations Flood et al derived the following equation.

$$RT \ln a_{FeO} = RT \ln N_{O^{2-}} . N_{Fe^{2+}} + N'_{Ca^{2+}} . N'_{SiO_4^{4-}} . \Delta G \quad \ldots(1)$$

where N' are the electrically equivalent ion fraction and ΔG is the free energy change for the reaction

$$FeO + \tfrac{1}{2}(2CaO.SiO_2) = CaO + \tfrac{1}{2}(2FeO.SiO_2) \quad \ldots\ldots\ldots \ (2)$$

Equation (1) can be extended to include additions of MnO and MgO and ferrous oxide activities have been calculated for basic steel-making slags and have been found to agree well with measured activities [21]. The above treatment can not be used for slags more acid than the orthosilicate join because at the orthosilicate join the calculated oxygen ion fraction is zero.

Lumsden has proposed a regular solution to enable activities in ternaries to be calculated from the corresponding binary activities [23]. This model considers a solution of two basic oxides to consist of a matrix of O^{2-} anions with randomly occupied interstitial cation sites. It suggests that when a small amount of silica is added to this solution, O^{2-} ions will add to the matrix while Si^{4-} ions will occupy the cation sites in a random manner like the basic oxide cations. This theory means that there will be ideal entropy of mixing but not necessarily zero enthalpy of mixing. In other words, the oxides will form a regular solution. As greater amounts of SiO_2 are added, complex anionic groupings of Si and O will be more likely to form and the regular solution model will break down. Thus the theory appears to be promising for the highly basic oxide melts where Richardson's theory does not hold. Lumsden has applied his theory to the ternary systems $FeO-Fe_2O_3-SiO_2$ which he considered as $FeO-FeO_{1.5}-SiO_2$ and obtained results which compare well with the experimental results determined by Michal and Schumann [17].

The above is a brief survey of the work that has been carried out on binary and ternary systems and the models that have been produced from these data. A great deal more work remains to be done and in the present work, the activities of silica in the ternary oxide systems $CaO-MgO-SiO_2$ and $MgO-Al_2O_3-SiO_2$ have been determined and the activities of the other two components calculated using Schumann's application of the Gibbs-Duhem equation. The results obtained in the $CaO-MgO-SiO_2$ system have been examined with regard to Richardson's model.

In the present work, compacts containing silica, graphite and silicon carbide were placed in a graphite crucible and allowed to come to equilibrium with carbon monoxide at 1500°C and 1550°C as represented by the following equation

$$SiO_2(\overset{\beta}{crist.}) + 3C(gr.) = SiC(cub.) + 2CO(g) \quad \ldots\ldots \quad (3)$$

This reaction must be considered as the summation of two other reactions

$$SiO_2(\overset{\beta}{crist.}) + C(gr.) = SiO(g) + CO(g) \quad \ldots\ldots\ldots \quad (4)$$

$$SiO(g) + 2C(gr.) = SiC(cub.) + CO(g) \quad \ldots\ldots\ldots \quad (5)$$

The equilibrium pressure ($pCO + pSiO$) was measured at 1500°C and 1550°C. Silica, graphite and silicon carbide were all in their standard states therefore the equilibrium constant for reaction (3) $K_3 = p^{2}CO(\text{standard})$. The partial pressure of carbon monoxide in the system pCO was obtained from the measure equilibrium pressure ($pCO + pSiO$) and the equilibrium constant for reaction (4), $K_4 = pSiO.pCO$. Substitution of a compact containing the slag yields values of pCO(slag), this being obtained from the measured reaction pressure at equilibrium ($pCO + pSiO$) and the equilibrium constant for reaction (5), $K_s = \frac{pCO}{pSiO}$. The silica activity of the slag, referred to the standard state of β cristobalite, is given by $p^s CO(slag)/p^s CO(standard)$.

CHAPTER II

APPARATUS AND EXPERIMENTAL PROCEDURE

APPARATUS AND EXPERIMENTAL PROCEDURE

General Apparatus

The apparatus used is shown in Figure 1 and is essentially that used by Kay and Taylor [5] with a few minor modifications. These modifications are as follows.

(1) Glass tubing B replaces copper tubing. This was found necessary because the copper tubing was connected to the manometer A and the two glass stop-cocks by polythene tubing to form vacuum-tight joins and it was found that leaks developed easily in these joins. Replacement of the entire unit in glass eliminated six possible sources of leaks.

(2) O-ring seal C on mullite sheath H replaces an apiezon wax seal. This enables the sheath to be replaced with far less trouble.

(3) The Kelvin-Hughes temperature controller replaces an older model to give more sensitive control.

It is considered that the diagram of the apparatus is self-explanatory.

Temperature measurement and control

The temperature of the slag under investigation was measured by a Cambridge potentiometer and a Pt Pt.13%Rh thermocouple G which was placed inside a mullite sheath H, the join of the

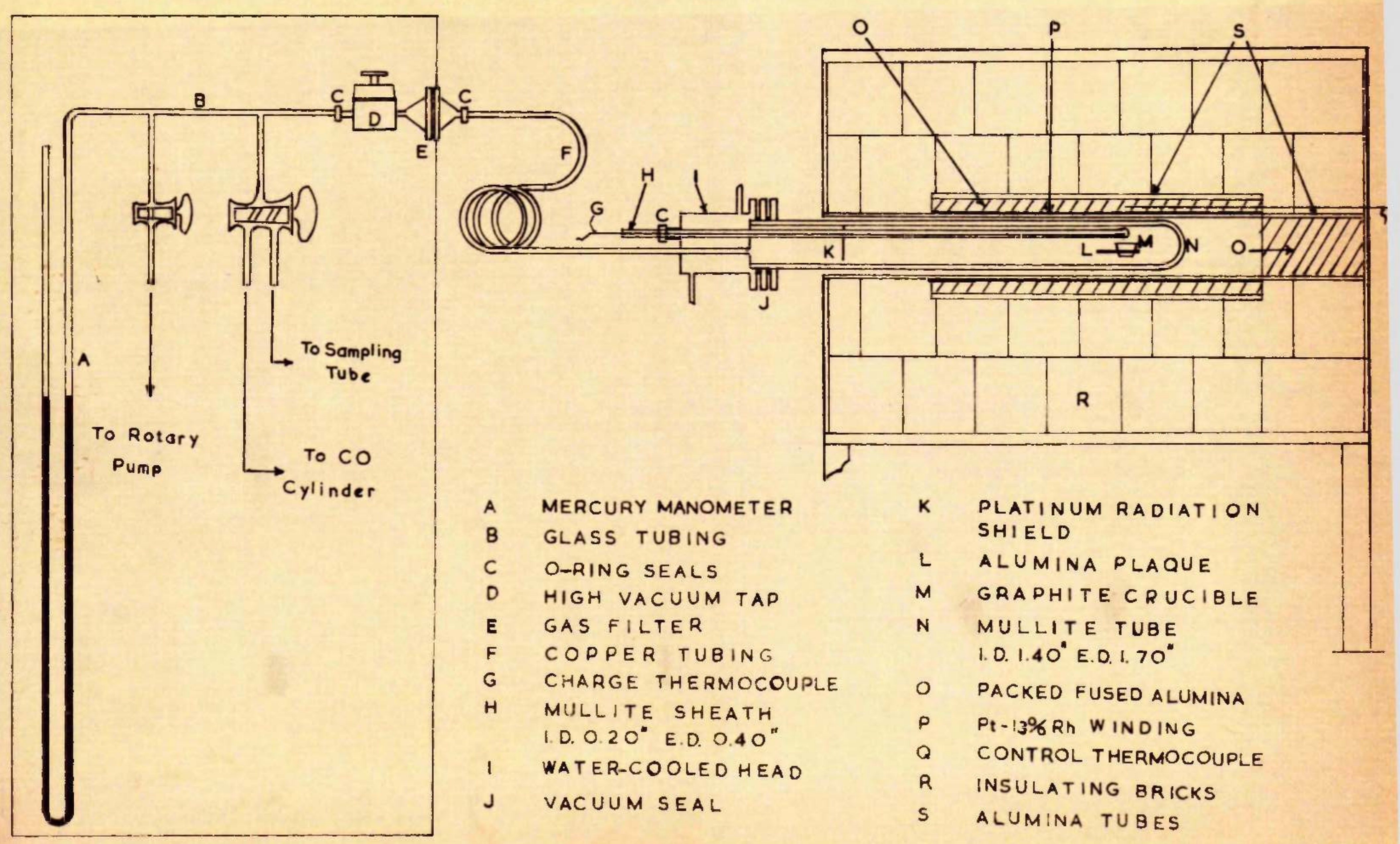

A	MERCURY MANOMETER
B	GLASS TUBING
C	O-RING SEALS
D	HIGH VACUUM TAP
E	GAS FILTER
F	COPPER TUBING
G	CHARGE THERMOCOUPLE
H	MULLITE SHEATH I.D. 0.20" E.D. 0.40"
I	WATER-COOLED HEAD
J	VACUUM SEAL
K	PLATINUM RADIATION SHIELD
L	ALUMINA PLAQUE
M	GRAPHITE CRUCIBLE
N	MULLITE TUBE I.D. 1.40" E.D. 1.70"
O	PACKED FUSED ALUMINA
P	Pt-13% Rh WINDING
Q	CONTROL THERMOCOUPLE
R	INSULATING BRICKS
S	ALUMINA TUBES

FIG 1 — DIAGRAM OF APPARATUS

thermocouple being situated directly above the crucible containing the slag compact. The combination of potentiometer and thermocouple was standardised frequently against the melting point of palladium (1552°C). This standardisation was considered to be satisfactory over the experimental temperature range (1500-1550°C).

A Kelvin-Hughes electronic on/off controller with proportional action was used in conjunction with Pt/Pt-13%Rh control thermocouple placed next to furnace winding to control the furnace temperature automatically. This temperature controller gave a considerable amount of trouble. It was found that voltage fluctuations in the main supply caused corresponding shifts in the temperature at which the device was controlling. A constant voltage transformer was obtained and placed in the circuit to deal with this problem. The device now controlled the temperature to about ± 2° - ± 3°C but over the period of a run, say 5 - 6 hours, the mean temperature dropped slowly by about 10°C. This meant that the controller required constant adjustment to keep the furnace temperature constant at 1500°C or 1550°C. Eventually the technique was developed of checking the temperature every 15 minutes and adjusting the controller if necessary, and as gas equilibrium was approached the temperature would be watched constantly. This technique proved satisfactory but tiresome as it was very easy to over-adjust the controller. Also this problem frequently meant an increase in the time taken to a run because it was sometimes difficult to determine whether a small change in the gas pressure was due to the fact that equilibrium had not yet been reached or due to a small change in the furnace temperature.

Leaks

Initially a certain amount of trouble was experienced in keeping the system gas-tight but this was soon traced to the copper/polythene and polythene/glass joins as mentioned previously. When the copper tubing was replaced by glass tubing this problem was eliminated.

It was now found that when the glass stop-cocks were greased regularly, leaks developed only in the mullite tube N and/or sheath H, both of which became porous after a number of runs. The mullite tubes and sheaths were found to vary in the length of time that they remained gas-tight. The sheaths did not last as long as the tubes, the sheaths being thinner by one third. They also tended to droop at the end and touch the graphite crucible. When this happened they became porous very quickly. To reduce the possibility of this happening, the sheath was rotated through 90° after each run.

Sometimes during a run it was found that it would be difficult to determine whether or not a leak had developed. For example, if gas was being evolved in the system in order to reach equilibrium below atmospheric pressure, a leak would only add to the gas pressure and a long time could be spent measuring the rate of change of gas pressure before a leak was suspected. The slow rate of reaction which was experienced meant that there was a greater possibility of the sheath drooping to touch the graphite crucible and thus a greater possibility of a leak developing. If a leak did develop during a run then that run was rejected.

Crucible and Support

The slag compact was contained in a graphite crucible 5/8" in height, upper and lower external diameters were 1.1/8" and 7/8" respectively while crucible thickness was 1/16" and approximate weight was 6 gm. The graphite crucible was placed in an alumina plaque to prevent contact between graphite and the mullite tube. A lid was provided with each crucible to prevent the free diffusion of SiO gas from the crucible contents. This was necessary because condensation of SiO at the cooler end of the tube takes place and a continual removal of SiO from the compact would alter the measured silica content. Even with the lid, a small amount of deposit was normally found after each run and removed. This deposit consisted of a finely divided mixture of graphite, silica and silicon carbide indicating that the SiO had been reoxidised by the CO at the cooler end of the tube. It was not considered that this deposit was sufficient to alter the silica content of the slag appreciably.

The crucible and lid were machined from Acheson's AGR quality graphite and degassed by placing on the alumina plaque inside the mullite tube and evacuating for 3 hours at 1550°C. Initially this method proved satisfactory but a new batch of AGR graphite was found to evolve gas even after this treatment. Extension of the evacuation period did not produce satisfactory results and a denser quality of graphite, AGW, was obtained. This was successfully degassed by evacuating at 2150°C for 3 hours using a high frequency induction coil.

Slag Compacts

Master slags were made up from the following materials.

1) Ground, acid washed quartz sand.

2) Analar calcium carbonate.

3) Analar magnesia, after ignition for 3 hours at 1000°C.

4) Analar alumina, after ignition for 1 hour at 1000°C.

All the above constituents were passed through a 200 mesh sieve. The acid-washed sand was also used for the standard silica runs.

The slag constituents were carefully weighed out and carefully mixed by hand before melting in a graphite crucible using high frequency induction heating. Melting of the $CaO-MgO-SiO_2$ slags required care because the lime was present as calcium carbonate and carbon dioxide had to be removed. This could cause 'puffing' if heating was too rapid and so loss of slag. If this happened the slag was rejected. The molten slag was cast, crushed in the percussion mortar and ground in the agate mortar to pass through a 200 mesh sieve.

Analysis of the master slags so produced proved to be unsatisfactory and examination of the literature and advice from a commercial concern brought the conclusion that 'made-up' analysis, i.e. the analysis obtained by carefully weighing out the constituents, would be more reliable. An occasional 'check' analysis was carried out to confirm any doubtful slag and all analyses quoted in Table I are obtained from the weigh-out figures.

The slag compacts used were made up from the master slags or the acid-washed sand (-200 mesh), previously degassed AGW graphite (-200 mesh) and commercial silicon carbide (-700 mesh). 4 gm. of slag or sand were carefully mixed by hand with 1 gm. of graphite and then ground together for 15 minutes in the agate mortar to give

TABLE 1. Analyses of Master Slags

	Composition (Weight Percent)			
Slag	CaO	MgO	Al_2O_3	SiO_2
A	30·0	10·0	-	60·0
B	50·0	10·0	-	40·0
C	15·0	20·0	-	65·0
D	40·0	20·0	-	40·0
E	10·0	30·0	-	60·0
F	25·0	30·0	-	45·0
G	-	24·0	10·0	66·0
H	-	32·0	10·0	58·0
I	-	7·0	20·0	73·0
J	-	30·0	20·0	50·0
K	-	14·0	30·0	56·0
L	-	22·0	30·0	48·0

intimate mixing. The silicon carbide was then mixed in by hand as thoroughly as possible. The silicon carbide was not added to the agate mortar as there was the possibility that its abrasive properties might increase the silica content of the slag from the agate. A little water was now added to the powder and it was compacted by applying a pressure of 25 tons/sq.in. The compact was dried in an oven at 110° - 120°C for 12 hours.

Determination of the Equilibrium Reaction Pressure

A new mullite tube and sheath were degassed by evacuating for two hours at 1550°C, the temperature then being dropped to 1000°C.

The slag compact was then placed in position in the graphite crucible inside the furnace tube at 1000°C and the system was evacuated for 1/2 hour while the temperature was being raised to 1100°C. Carbon monoxide was now introduced into the system to the approximate equilibrium pressure and the temperature raised to 1550°C over a period of 2 - 2.1/2 hours. The controller was now adjusted slightly to give a temperature of exactly 1550°C and carbon monoxide was replaced by momentarily evacuating the system and again introducing carbon monoxide from the cylinder.

The rate of change in the CO pressure was now noted carefully and if this was rapid CO was either admitted or withdrawn in order to bring the pressure closer to the equilibrium pressure. When the pressure had remained constant for a certain period of time, 1/2 hour for most slags but increasing for the more acid slags to 2 hours for standard silica compacts, it was decided equilibrium had been reached. With some runs, e.g. if time taken to reach equilibrium had been excessive, say 3 - 4 hours, or if the graphite crucible was being used for the first run, the system would be momentarily evacuated and CO replaced to approach equilibrium again from the same side. This was to check for evolution of gas from the tube or the graphite crucible. Very occasionally the equilibrium readings did not match and equilibrium was approached for the third time from the same side. In every case no further pressure change was observed.

If the initial equilibrium pressure reading had been reached fairly rapidly, say 1 - 2 hours, and if the graphite crucible had been used previously, then the system would be momentarily evacuated, CO admitted and equilibrium approached from the other side. Again when equilibrium was reached the CO could be replaced and equilibrium again approached as before. Thus the equilibrium pressure was determined from 'above' and 'below' by this procedure and the mean taken.

Throughout the run it was necessary to make slight adjustments to the controller in order to maintain a steady temperature.

If circumstances allowed the temperature was then dropped to 1500°C and the above procedure was repeated. Usually it was necessary to lower the temperature to 1000°C overnight and carry out the run at 1500°C on the following day. If this was the case, the system was opened to the atmosphere, any furnace deposit removed, position of the charge checked, mullite sheath rotated through 90° and procedure carried out as before.

Experimental Accuracy

A true estimation of experimental accuracy can only be made when the experiment is repeated a number of times and the standard deviation is calculated. The larger the number of times the experiment is repeated, the more reliable is the estimation of the experimental accuracy. In the present work, in common with other work of this nature, only one measurement was made on any one slag at one temperature. Thus it is not possible to get a true estimation of experimental accuracy. It is possible, however, to determine the precision with which measurements can be made in this work.

There are two main sources of error, i.e. the temperature measurements and the measurement of the equilibrium pressure. The standarisation of the potentiometer with a Pt/Pt-13% Rh thermocouple against the melting point of palladium (1552°C) and the measurement of the cold junction temperature were both taken into account and it is considered that the temperature can be measured accurately to ± 3°C. The equilibrium pressure was measured from 'above' and 'below' and the average difference in readings was approximately 1 cm. Hg.The accuracy with which the manometer and barometer can be read is considered to be negligible in comparison with the above difference and the equilibrium pressure is considered accurate to ± 0·5 cm. Both the above factors were taken into account and the accuracy of the silica activities estimated at ± 4%.

CHAPTER III

RESULTS

RESULTS

STANDARD SILICA RUNS

Three runs were carried out at both 1500 and 1550°C with compacts containing pure silica

$$SiO_2(\overset{\beta}{\text{crist.}}) + 3C(gr) = SiC(cub.) + 2CO(g) \quad \ldots \quad (3)$$

The equilibrium partial pressure of carbon monoxide obtained are given in Table 2.

These values were obtained from the measured equilibrium pressures ($pCO + pSiO$) and the free energy change for reaction (4)

$$SiO_2(\overset{\beta}{\text{crist.}}) + C(gr) = CO(g) + SiO(g) \quad \ldots \quad (4)$$

This free energy change is given by equation (D) in the appendix as

$$\Delta_4 G^\circ_T = +158{,}700 - 79{\cdot}06\,T \text{ cal./mol.} \qquad (1686 - 1900^\circ K)$$

Both cristobalite and graphite are in their standard states, therefore the equilibrium constant for reaction (4) reduces to $K_4 = pCO.pSiO$. Values of this constant were obtained from equation (D) at different temperatures and are given in Table 3. A plot of $\log pCO.pSiO$ against $1/T^\circ K$ is shown in Figure 3. The measured reaction pressure ($pCO + pSiO$) is approximated to pCO, $pSiO$ obtained from $pCO.pSiO$ and thus pCO determined.

TABLE 2. Equilibrium partial pressures of carbon monoxide for SiO_2 (crist.) + C (graph) + SiC (cub.) compacts.

Run	pCO + pSiO atm.	pCO atm.	T°K	$^1/_{T°K} \times 10^5$	$\log_{10} pCO$
1	0·863	0·856	1776·5	56·25	-0·067
	1·350	1·337	1822·0	54·9	0·129
2	0·800	0·793	1774·0	56·35	-0·111
	1·396	1·383	1822·0	54·9	0·141
3	0·771	0·764	1774·0	56·35	-0·117
	1·356	1·342	1822·5	54·85	0·128

FIG. 2

$SiO_2 + 3C = SiC + 2CO$

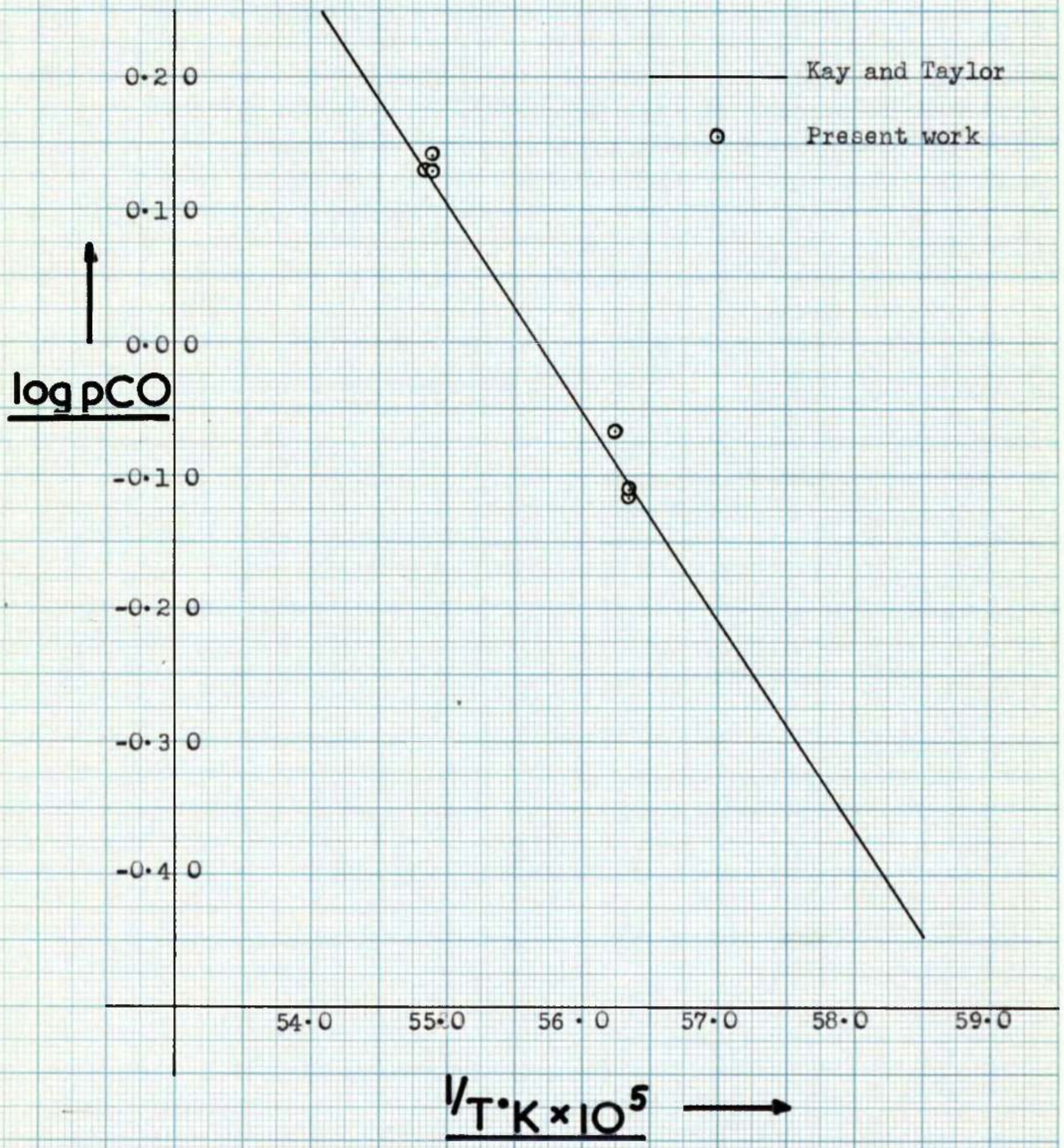

TABLE 3 Equilibrium constants for the reaction

SiO_2 (β crist.) + C(gr) = SiO(g) + CO(g)

T°K	$\frac{1}{T°K}$	K	log K
1723	58·0	$1·45 \times 10^{-3}$	-2·84
1773	56·4	$5·25 \times 10^{-3}$	-2·28
1823	54·8	$1·89 \times 10^{-2}$	-1·723

TABLE 4 Equilibrium constants for the reaction

SiO(g) + 2C(gr) = SiC(cub.) + CO(g).

T°K	$\frac{1}{T°K}$	K	log K
1723	58·0	$1·22 \times 10^{2}$	2·085
1773	56·4	$1·10 \times 10^{2}$	2·04
1823	54·8	$9·89 \times 10^{2}$	1·995

FIG. 3

$SiO_2 + C = CO + SiO$

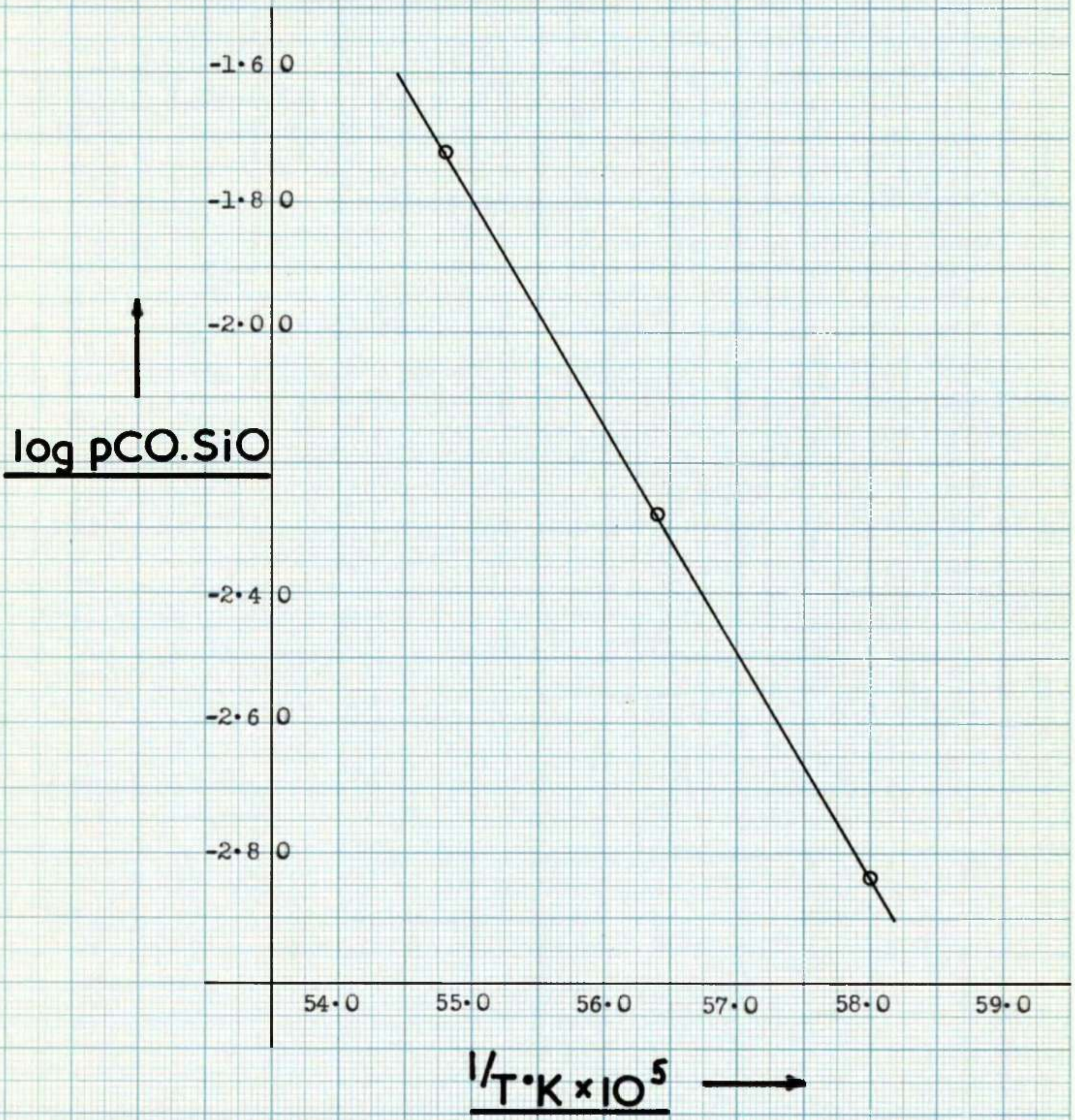

FIG. 4

$SiO + 2C = SiC + CO$

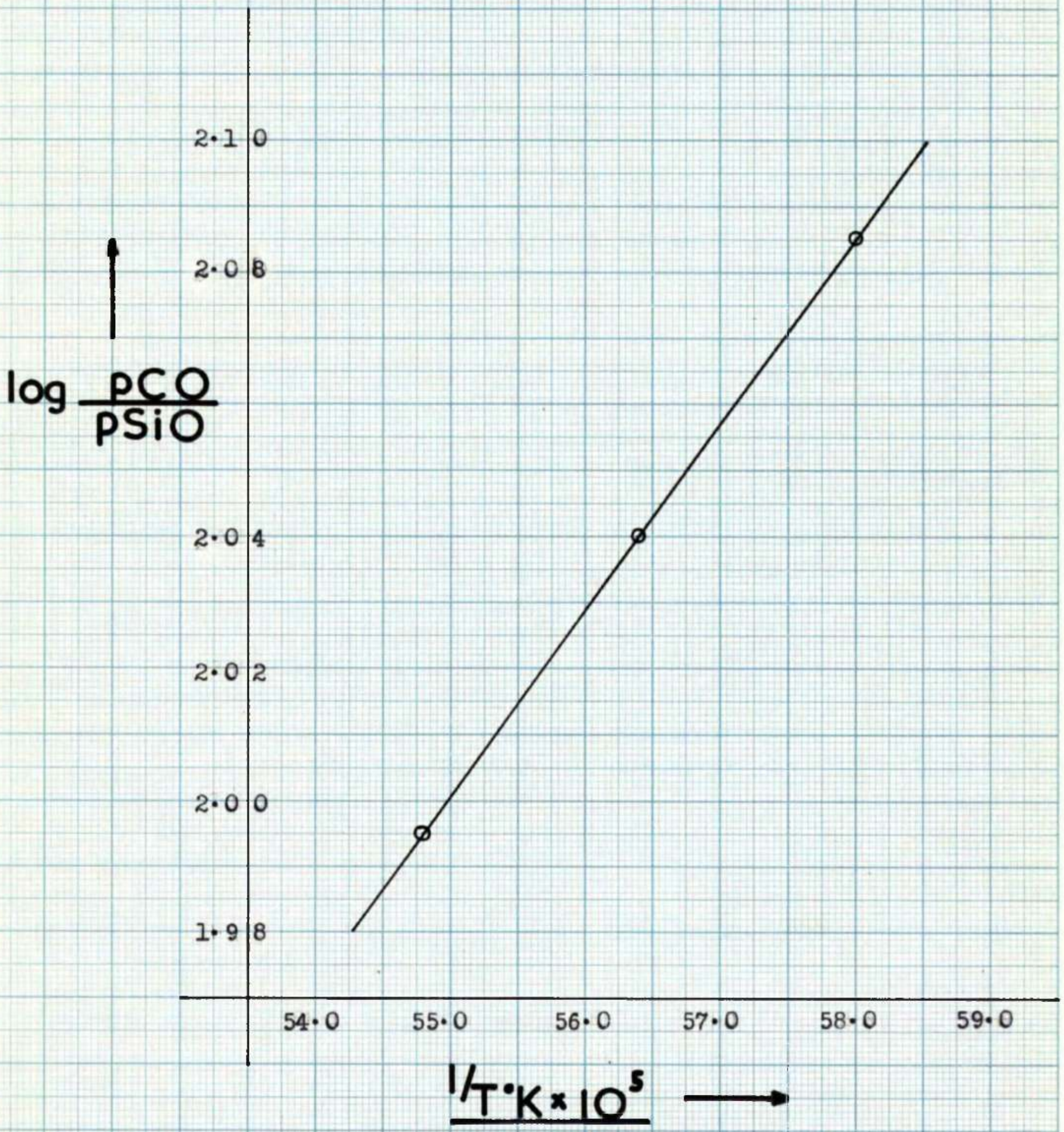

The values obtained for the partial pressures of carbon monoxide have been plotted as log pCO against $1/_T$°K and are shown in Figure 2 with the straight line obtained by Kay and Taylor [5] for this reaction. As can be seen, the pressures obtained in the present work confirm the values obtained by Kay and Taylor, therefore, it was decided to accept the experimental results determined by these workers and use them as the standard from which activities were determined in the present investigation.

Since the publication of the work by Kay and Taylor new data on the free energy of formation of silica [39, 40] have become available. The partial pressure of SiO and thus CO have been recalculated using this data and it is this slightly modified data that is shown in Figure 2. The linear equation for the straight line in Figure 2 now becomes

$$\log_{10} p\mathrm{CO} = -15{,}950/T + 8{\cdot}87 \qquad (1705 - 1828\,^\circ\mathrm{K}) \quad \ldots (6)$$

This equation was then used to obtain the free energy change for reaction (3)

$$\mathrm{SiO_2}(\overset{\beta}{\mathrm{crist.}}) + 3\mathrm{C(gr)} = \mathrm{SiC(cub.)} + 2\mathrm{CO(g)} \quad \ldots\ldots \qquad (3)$$

and this is given by

$$\Delta_3 G^{\circ}_{T} = +146{,}110 - 81{\cdot}3\,T \qquad \ldots\ldots\ldots\ldots \quad (7)$$

CALCULATION OF SILICA ACTIVITIES

Values of the equilibrium pressures ($p_{CO} + p_{SiO}$) have been determined over a number of compacts containing slags and the equilibrium partial pressure of carbon monoxide associated with the equation

$$SiO_2(slag) + 3C(gr.) = SiC(cub.) + 2CO(g) \quad ......(6)$$

was obtained from the measured equilibrium pressure ($p_{CO} + p_{SiO}$) and the free energy change for reaction (5)

$$SiO(g) + 2C(gr.) = SiC(cub.) + CO(g) \quad ..... \quad (5)$$

Both graphite and silicon carbide are in their standard states therefore the equilibrium constant reduces to $K_5 = p_{CO}/p_{SiO}$. The free energy change for reaction (5) is obtained from equation (7) and equation (D) in the appendix as

$$\Delta_5 G^\circ_T = -12,600 - 2\cdot24\ T \quad .... \quad (9)$$

Values of K_5 obtained from this equation are given in Table 4 at different temperatures. A plot of log p_{CO}/p_{SiO} against $1/_T$ °K is shown in Figure 4.

In the presence of solid graphite and silicon carbide the silica activity of any slag is given by

$$aSiO_2 = p^2CO(slag)/p^2CO(standard)$$

THE CaO-MgO-SiO$_2$ SYSTEM

The phase diagram for the system CaO-MgO-SiO$_2$ [25] is shown in Figure 5 and the silica activities of liquid slag at 1500 and 1550°C are given in Tables 5 and 6 and shown in Figures 6, 7, 8, 9 and 10.

Silica activities of liquid slags in the ternary were investigated at 1500 and 1550°C along lines of constant magnesia content, i.e. 10%, 20% and 30% magnesia by weight.

Silica activities of liquid slags in the CaO-SiO$_2$ binary have been determined by a number of workers as was mentioned in the Introduction. It was decided that the best data available was a slightly modified form of the data produced by Kay and Taylor [5], i.e. at the lime end of the binary, towards the extreme limit of available data, Kay and Taylor's results have been slightly modified in view of the results obtained by the other investigators [4, 6 and 7]. These results are included in Figures 9 and 10 and can be seen to be consistent with the data produced in the present work.

TABLE 5. Silica activities of CaO-MgO-SiO_2 slags

1500°C

Run	CaO	MgO	SiO_2	t°C	pCO+pSiO atm.	pCO atm.	$aSiO_2$
4	30·0	10·0	60·0	1499·5	0·717	0·711	0·875
5	36·7	10·0	53·3	1499·5	0·539	0·534	0·495
6	40·0	10·0	50·0	1499·5	0·470	0·466	0·375
7	43·3	10·0	46·7	1500	0·397	0·393	0·260
8	45·0	10·0	45·0	1500	0·374	0·370	0·230
9	47·5	10·0	42·5	1500	0·281	0·278	0·130
10	47·5	10·0	42·5	1500	0·302	0·299	0·150
11	40·0	10·0	50·0	1500	0·467	0·463	0·360
12	33·3	10·0	56·7	1500	0·625	0·619	0·645
13	15·0	20·0	65·0	1500	0·770	0·763	0·980
14	18·1	20·0	61·9	1500	0·724	0·717	0·865
15	23·3	20·0	56·7	1500	0·651	0·645	0·700
16	27·5	20·0	52·5	1500	0·551	0·546	0·500
17	31·7	20·0	48·3	1500	0·429	0·426	0·305
18	33·7	20·0	46·3	1500	0·369	0·366	0·225
19	38·0	20·0	42·0	1500	0·302	0·299	0·150
20	10·0	30·0	60·0	1500	0·747	0·740	0·920
21	12·5	30·0	57·5	1500	0·689	0·683	0·765
22	15·0	30·0	55·0	1500	0·606	0·600	0·605

TABLE 6 Silica activities of CaO-MgO-SiO$_2$ slags

1550°C

RUN	CaO	MgO	SiO$_2$	t°C	pCO+pSiO atm.	pCO atm.	aSiO$_2$
4	30·0	10·0	60·0	1548·0	1·180	1·168	0·765
5	36·7	10·0	53·3	1549·0	0·834	0·826	0·370
6	40·0	10·0	50·0	1548·5	0·725	0·718	0·285
7	43·3	10·0	46·7	1550	0·624	0·617	0·200
8	45·0	10·0	45·0	1550	0·575	0·569	0·170
9	47·5	10·0	42·5	1550	0·430	0·426	0·095
10	47·5	10·0	42·5	1550	0·395	0·391	0·080
11	40·0	10·0	50·0	1550	0·765	0·757	0·300
12	33·3	10·0	56·7	1550	1·037	1·025	0·550
13	15·0	20·0	65·0	1550	1·364	1·350	0·955
14	18·1	20·0	61·9	1550	1·233	1·220	0·780
15	23·3	20·0	56·7	1550	1·085	1·073	0·605
16	27·5	20·0	52·5	1550	0·899	0·890	0·415
17	31·7	20·0	48·3	1550	0·691	0·684	0·245
18	33·7	20·0	46·3	1550	0·640	0·633	0·210
19	38·0	20·0	42·0	1550	0·513	0·508	0·135
20	10·0	30·0	60·0	1550	1·243	1·230	0·795
21	12·5	30·0	57·5	1550	1·164	1·152	0·695
22	15·0	30·0	55·0	1550	1·030	1·020	0·545
23	17·5	30·0	52·5	1550	0·883	0·874	0·400
24	20·0	30·0	50·0	1550	0·718	0·711	0·265
25	22·5	30·0	47·5	1550	0·592	0·586	0·180
26	25·0	30·0	45·0	1550	0·503	0·498	0·130
27	-	39·0	61·0	1560	1·407	1·392	0·880
28	-	39·0	61·0	1570	1·541	1·526	0·790

FIG. 5

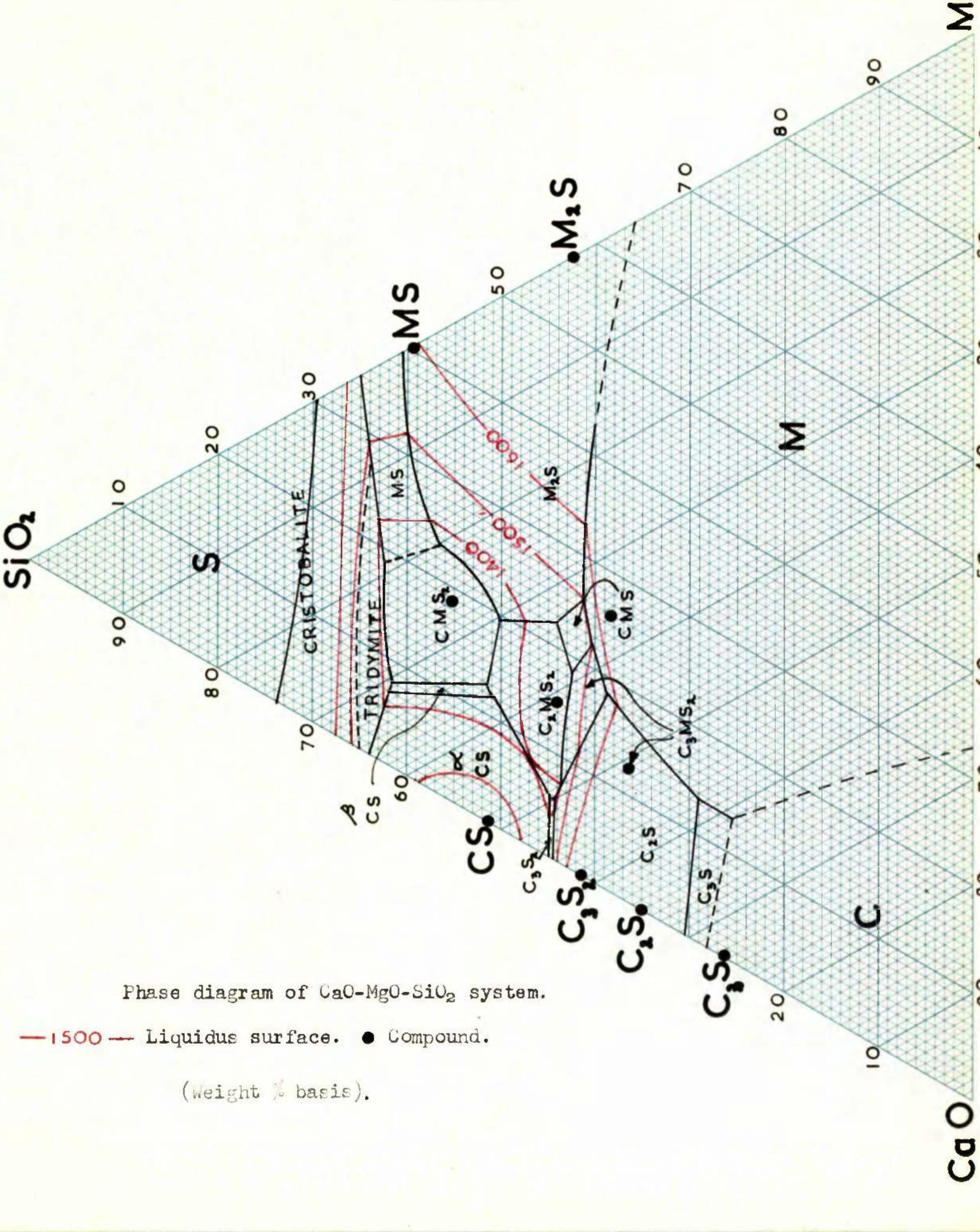

Phase diagram of CaO-MgO-SiO₂ system.

—1500— Liquidus surface. ● Compound.

(Weight % basis).

FIG. 6

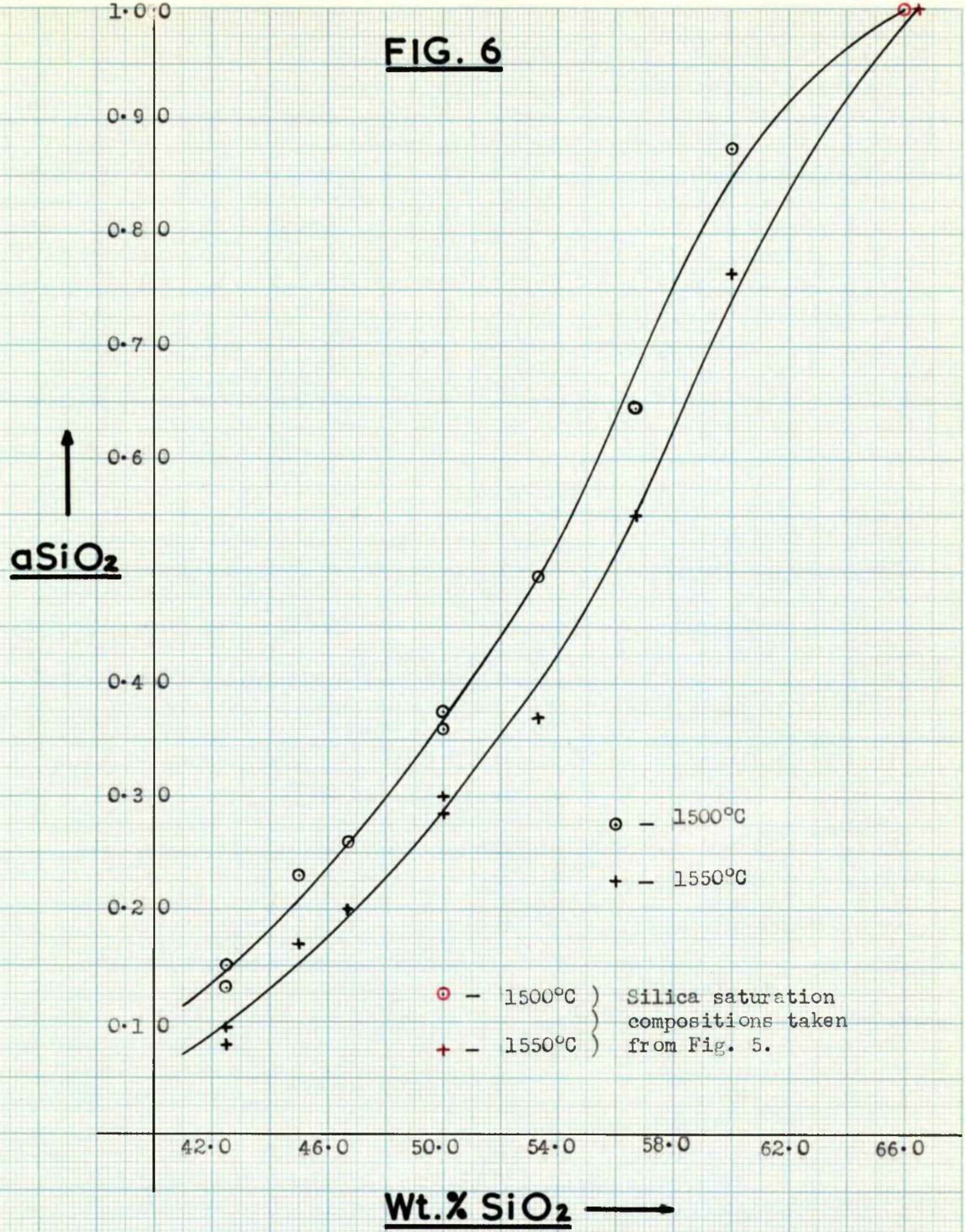

Silica activities of $CaO-MgO-SiO_2$ slags

(10% MgO)

FIG. 7

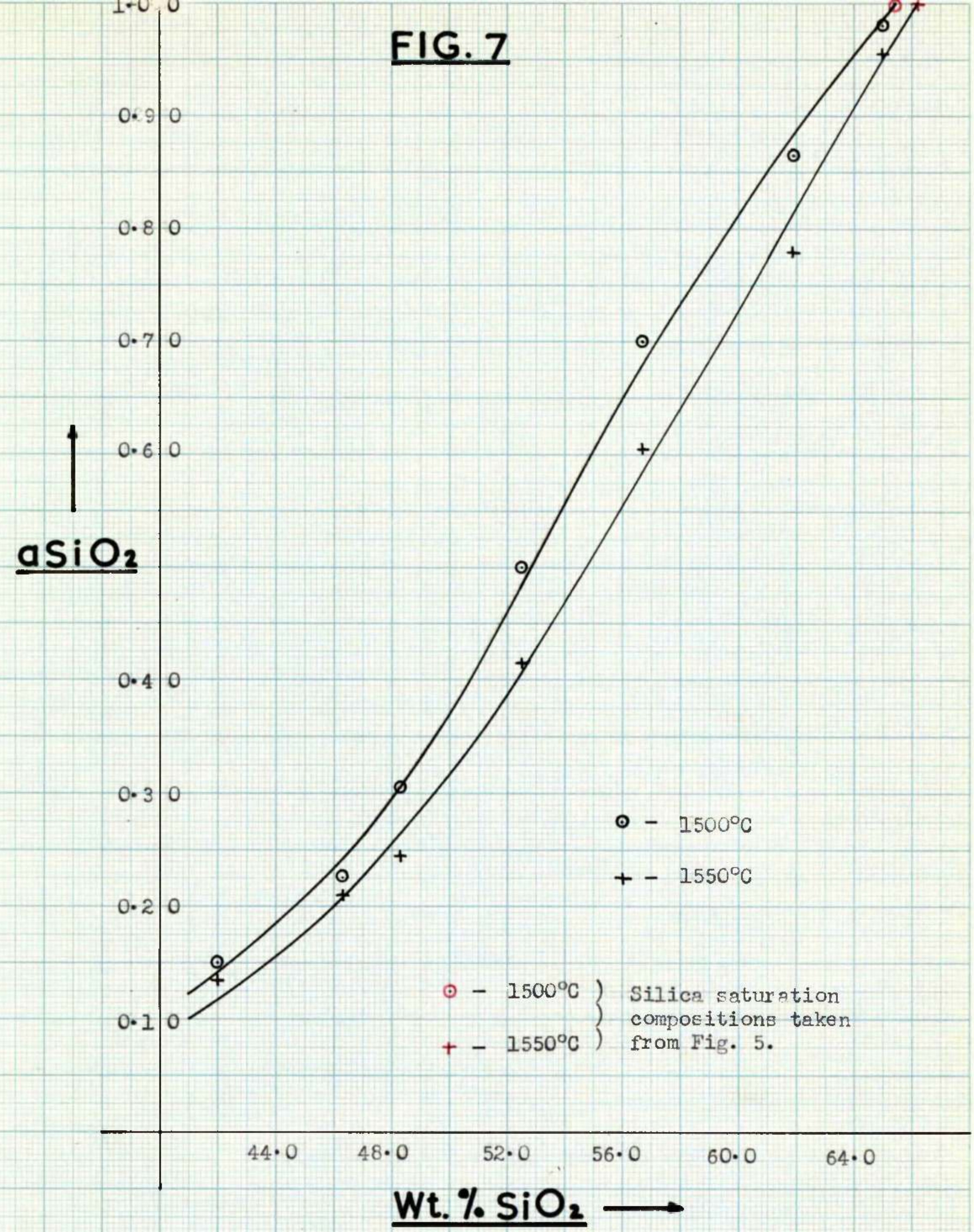

Silica saturation compositions taken from Fig. 5.

Silica activities of $CaO-MgO-SiO_2$ slags

(20% MgO)

FIG. 8

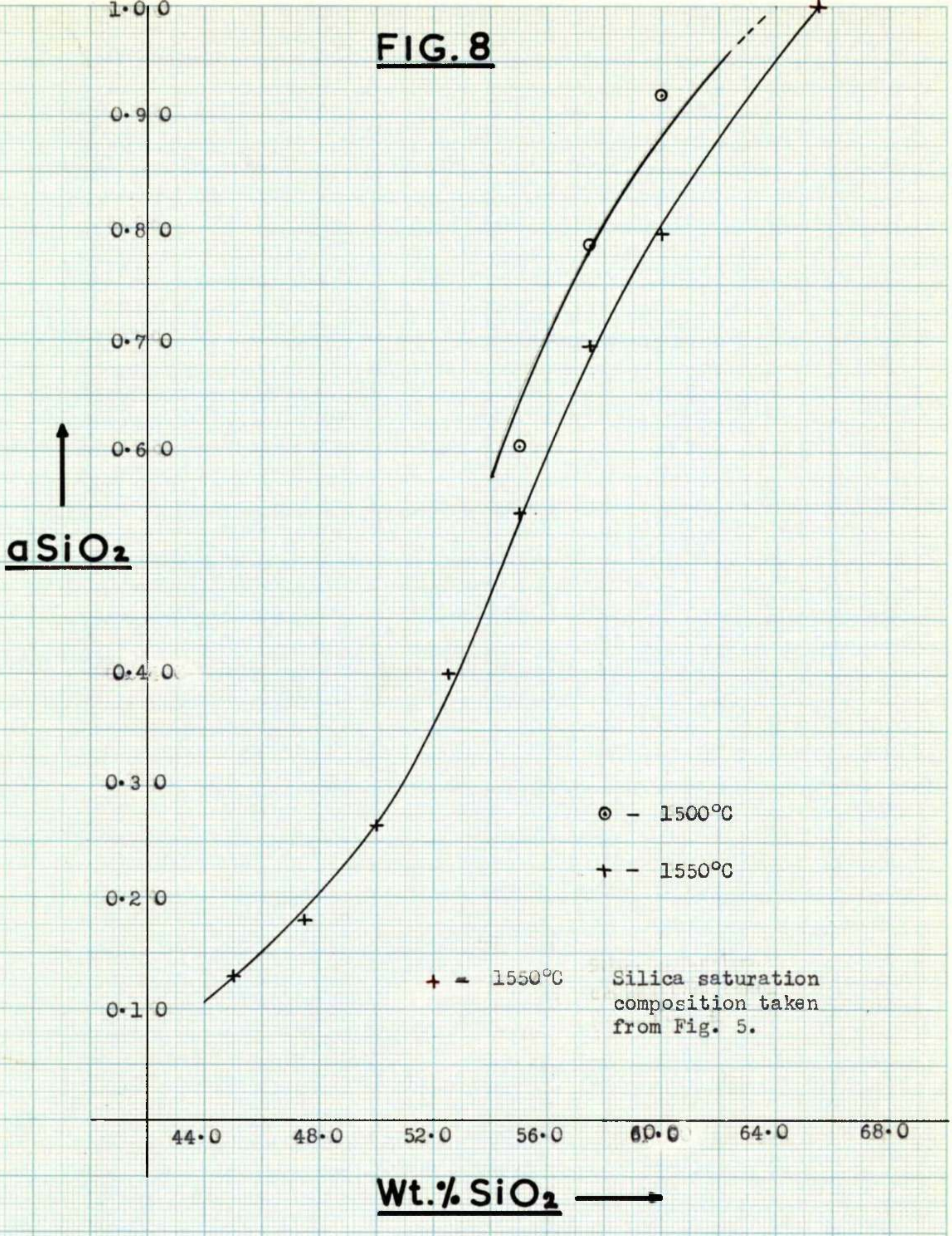

Silica activities of CaO-MgO-SiO_2 slags

(30% MgO)

FIG. 9

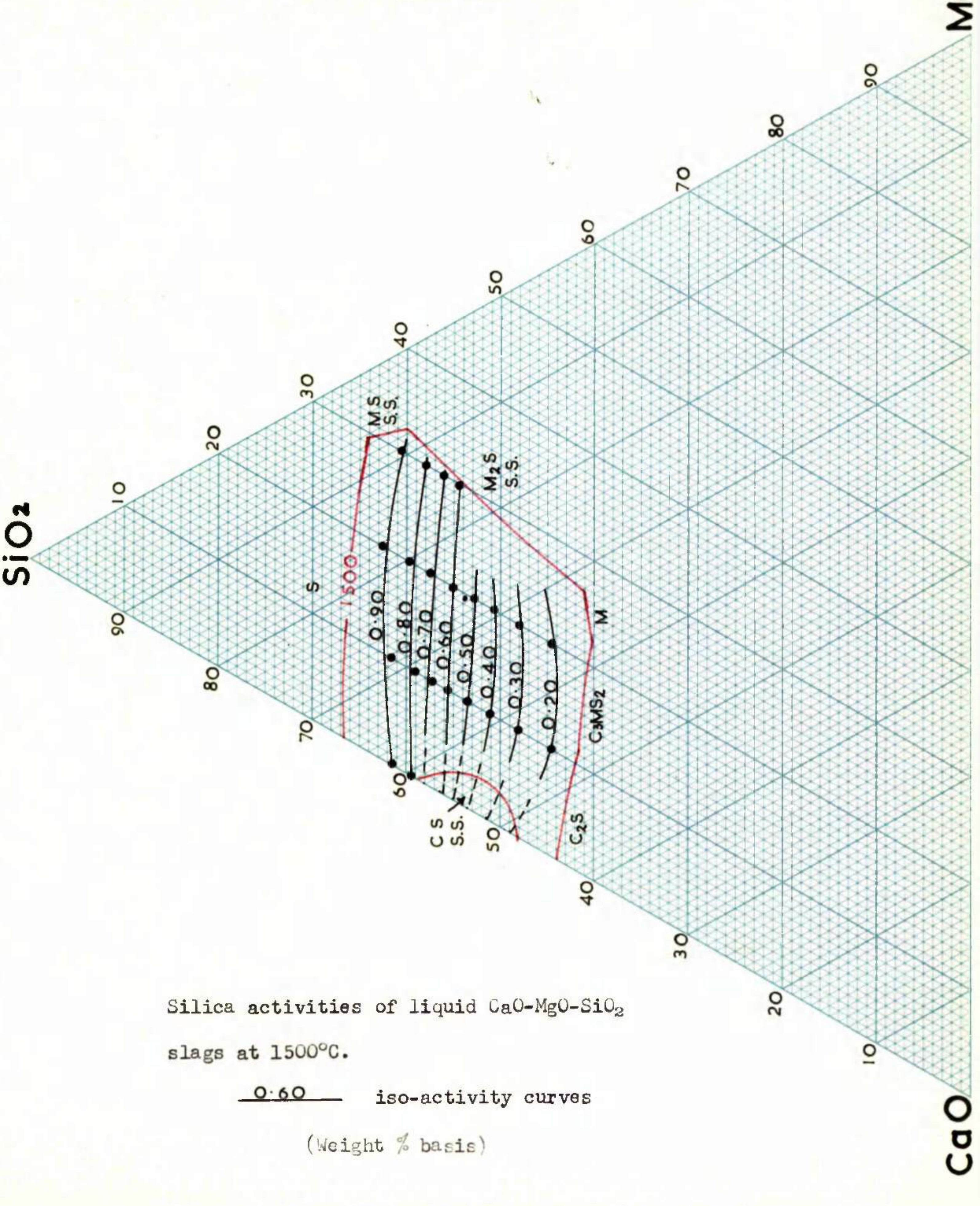

Silica activities of liquid CaO-MgO-SiO_2 slags at 1500°C.

0·60 iso-activity curves

(Weight % basis)

FIG. 10

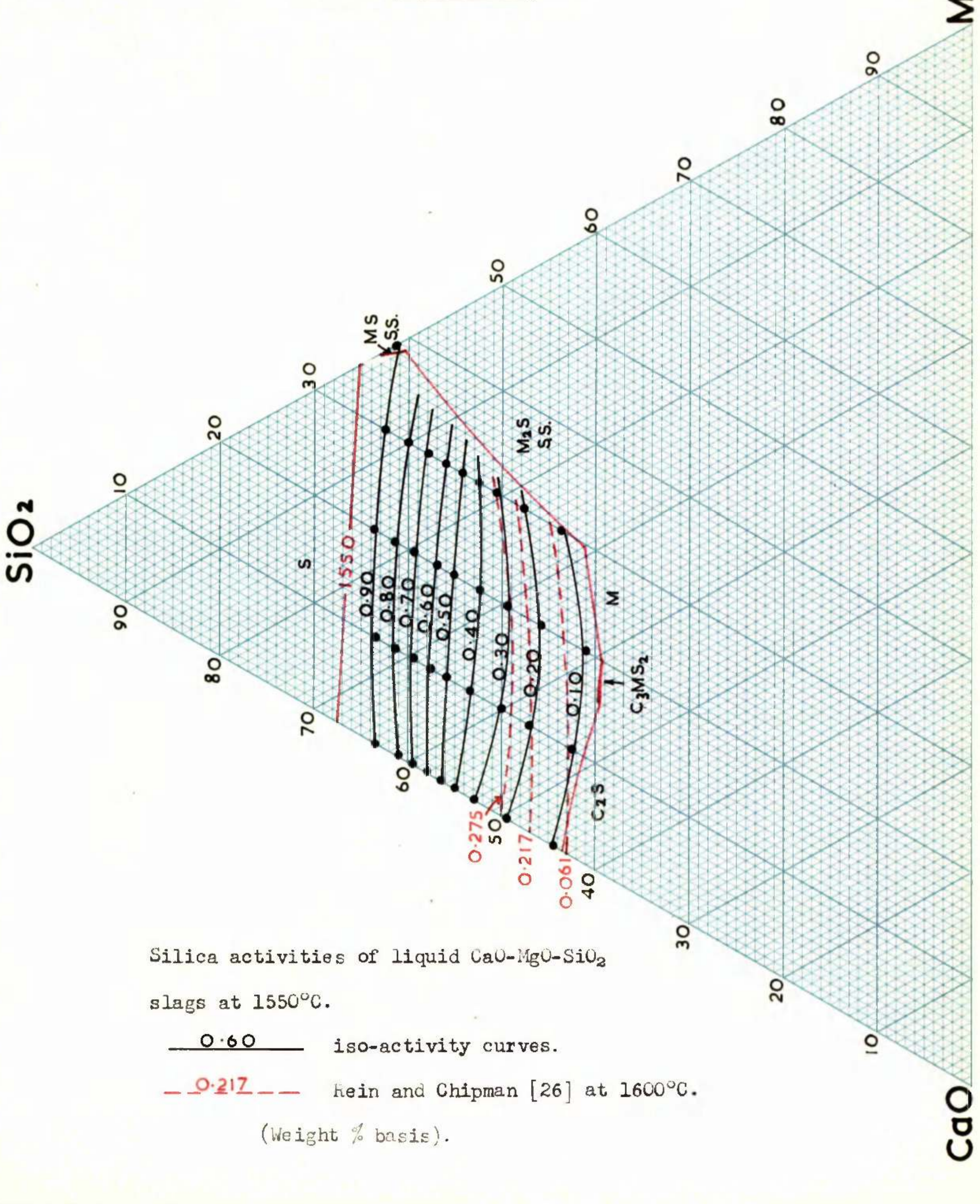

Silica activities of liquid CaO-MgO-SiO_2 slags at 1550°C.

0·60 iso-activity curves.

0·217 Rein and Chipman [26] at 1600°C.

(Weight % basis).

As examination of the phase diagram in Figure 5 shows that the high temperature required to obtain liquid melt on the $MgO-SiO_2$ binary severely restricts the determination of silica activities by the method used in the present work. In fact, only one point has been determined on the $MgO-SiO_2$ binary, i.e. the silica activity of the liquid slag at 61% SiO_2 was determined at 1560 and 1570°C and these activities were used to estimate the activity at 1550°C where the slag is solid. This was done by making use of the temperature coefficient obtained from the activity data determined at 1500°C and that at 1550°C. The silica activity of the slag at this point was taken as the mean of the activities obtained from 1560 and 1570°C. Two assumptions have been made in obtaining an estimation of the silica activity at this point on the $MgO-SiO_2$ binary, the first is that the activity of the solid slag at 1550°C is the same as if it were liquid, and secondly, the change of activity with temperature is constant. It is considered that as both these extrapolations are small then the possible error involved is also small and can be neglected.

THE $MgO-Al_2O_3-SiO_2$ SYSTEM

The phase diagram of the $MgO-Al_2O_3-SiO_2$ system [25] is shown in Figure 11. The silica activities of the liquid slags at 1500° and 1550°C are given in Tables 7 and 8 and are shown in Figures 12, 13, 14, 15 and 16.

Silica activities of liquid slags in the ternary were investigated along lines of constant alumina content, i.e. 10%, 20% and 30% alumina by weight.

Again there is only one silica activity determined on the MgO-SiO_2 binary, and no activity is available on the Al_2O_3-SiO_2 binary, the reason being obvious from examination of the phase diagram in Figure 11, i.e. silica activities can not be obtained due to the high temperature required to obtain liquid melts.

TABLE 7 Silica activities of $MgO-Al_2O_3-SiO_2$ slags

1500°C

Run	MgO	Al_2O_3	SiO_2	pCO + pSiO atm.	pCO atm.	$aSiO_2$
29	24·0	10·0	66·0	0·777	0·769	0·995
30	26·0	10·0	64·0	0·772	0·765	0·985
31	28·0	10·0	62·0	0·756	0·750	0·945
32	30·0	10·0	60·0	0·728	0·721	0·875
33	32·0	10·0	58·0	0·696	0·689	0·800
34	7·0	20·0	73·0	0·771	0·764	0·980
35	14·7	20·0	65·3	0·764	0·757	0·963
36	18·5	20·0	61·5	0·751	0·744	0·930
37	22·3	20·0	57·7	0·720	0·713	0·855
38	26·2	20·0	53·8	0·681	0·674	0·765
39	30·0	20·0	50·0	0·616	0·610	0·625
40	14·0	30·0	56·0	0·732	0·725	0·885
41	16·0	30·0	54·0	0·710	0·704	0·835
42	18·0	30·0	52·0	0·686	0·681	0·780
43	20·0	30·0	50·0	0·662	0·656	0·725
44	22·0	30·0	48·0	0·627	0·621	0·650

TABLE 8 Silica activities of $MgO-Al_2O_3-SiO_2$ slags

1550°C

Run	MgO	Al_2O_3	SiO_2	pCO + pSiO atm.	pCO atm.	$aSiO_2$
29	24	10·0	66·0	1·348	1·334	0·933
30	26·0	10·0	64·0	1·322	1·310	0·897
31	28·0	10·0	62·0	1·290	1·278	0·855
32	30·0	10·0	60·0	1·250	1·238	0·803
33	32·0	10·0	58·0	1·200	1·188	0·740
34	7·0	20·0	73·0	1·374	1·360	0·970
35	14·7	20·0	65·3	1·312	1·298	0·883
36	18·5	20·0	61·5	1·274	1·260	0·833
37	22·3	20·0	57·7	1·228	1·214	0·775
38	26·2	20·0	53·8	1·133	1·122	0·660
39	30·0	20·0	50·0	0·998	0·989	0·512
40	14·0	30·0	56·0	1·248	1·235	0·800
41	16·0	30·0	54·0	1·200	1·188	0·740
42	18·0	30·0	52·0	1·173	1·161	0·707
43	20·0	30·0	50·0	1·120	1·109	0·645
44	22·0	30·0	48·0	1·069	1·057	0·585

FIG. 11

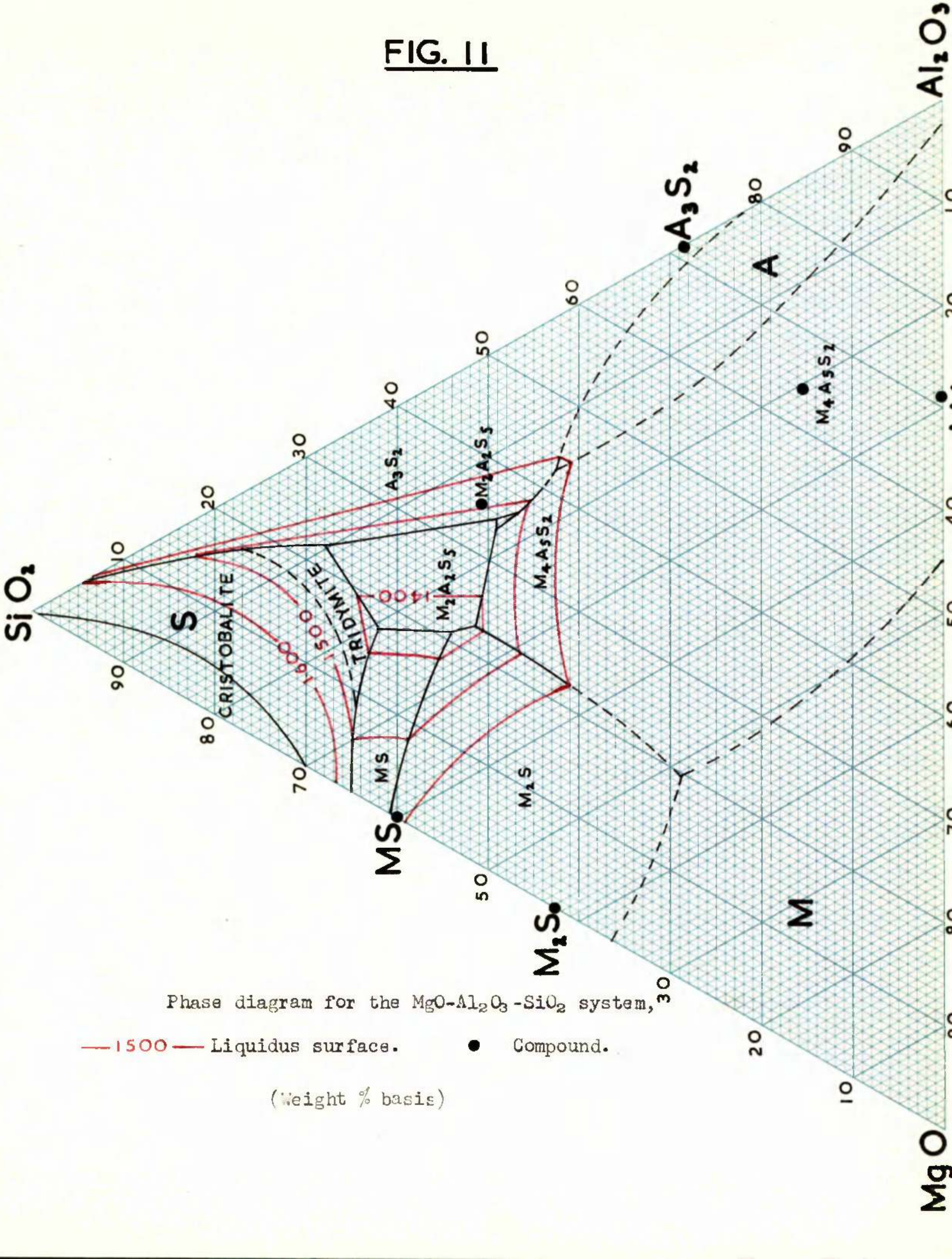

Phase diagram for the $MgO-Al_2O_3-SiO_2$ system,

—1500— Liquidus surface. ● Compound.

(Weight % basis)

FIG. 12

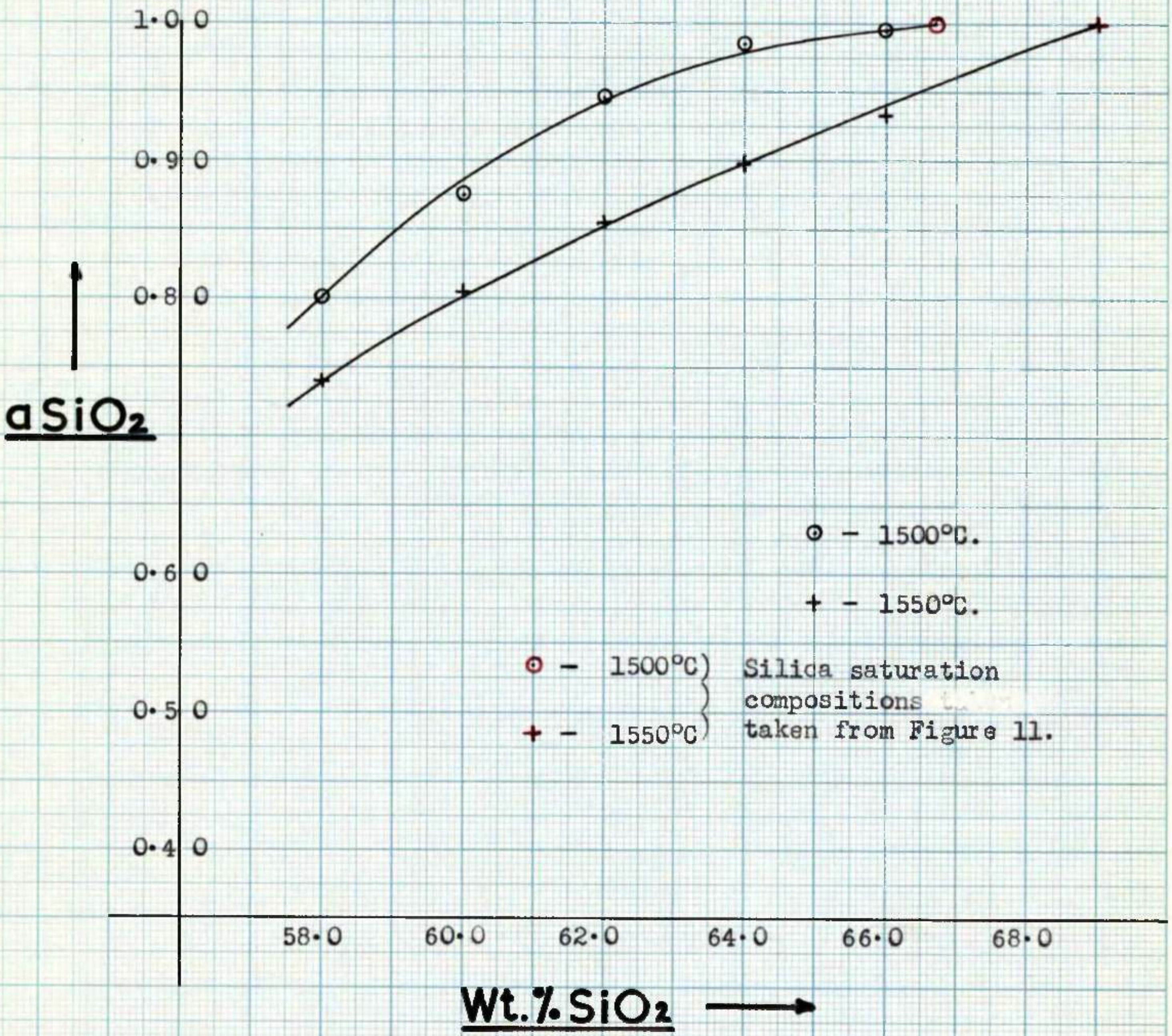

Silica activities of $MgO-Al_2O_3-SiO_2$ slags

(10% Al_2O_3)

FIG. 13

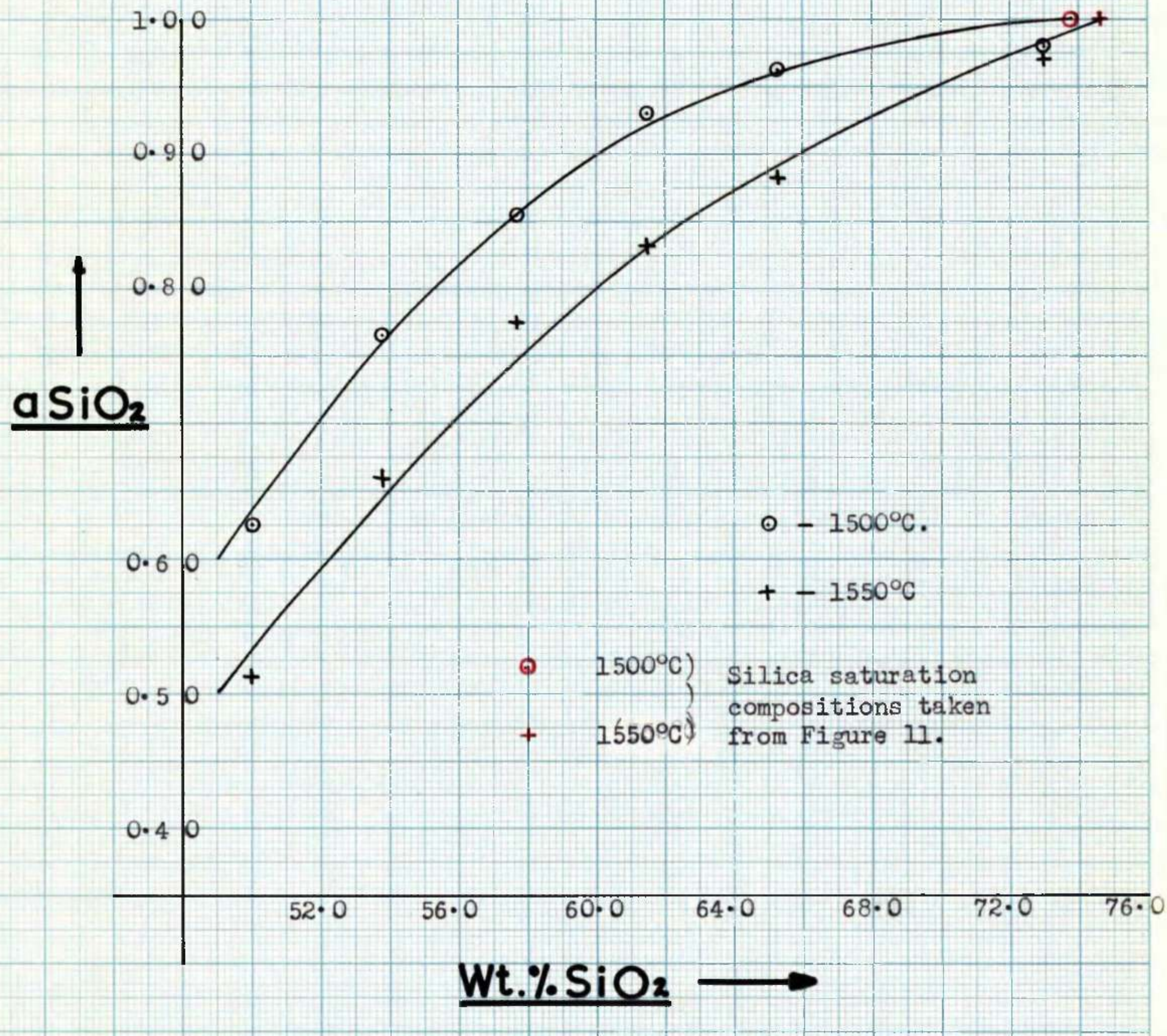

Silica activities of $MgO-Al_2O_3-SiO_2$ slags

($20\%\ Al_2O_3$)

FIG. 14

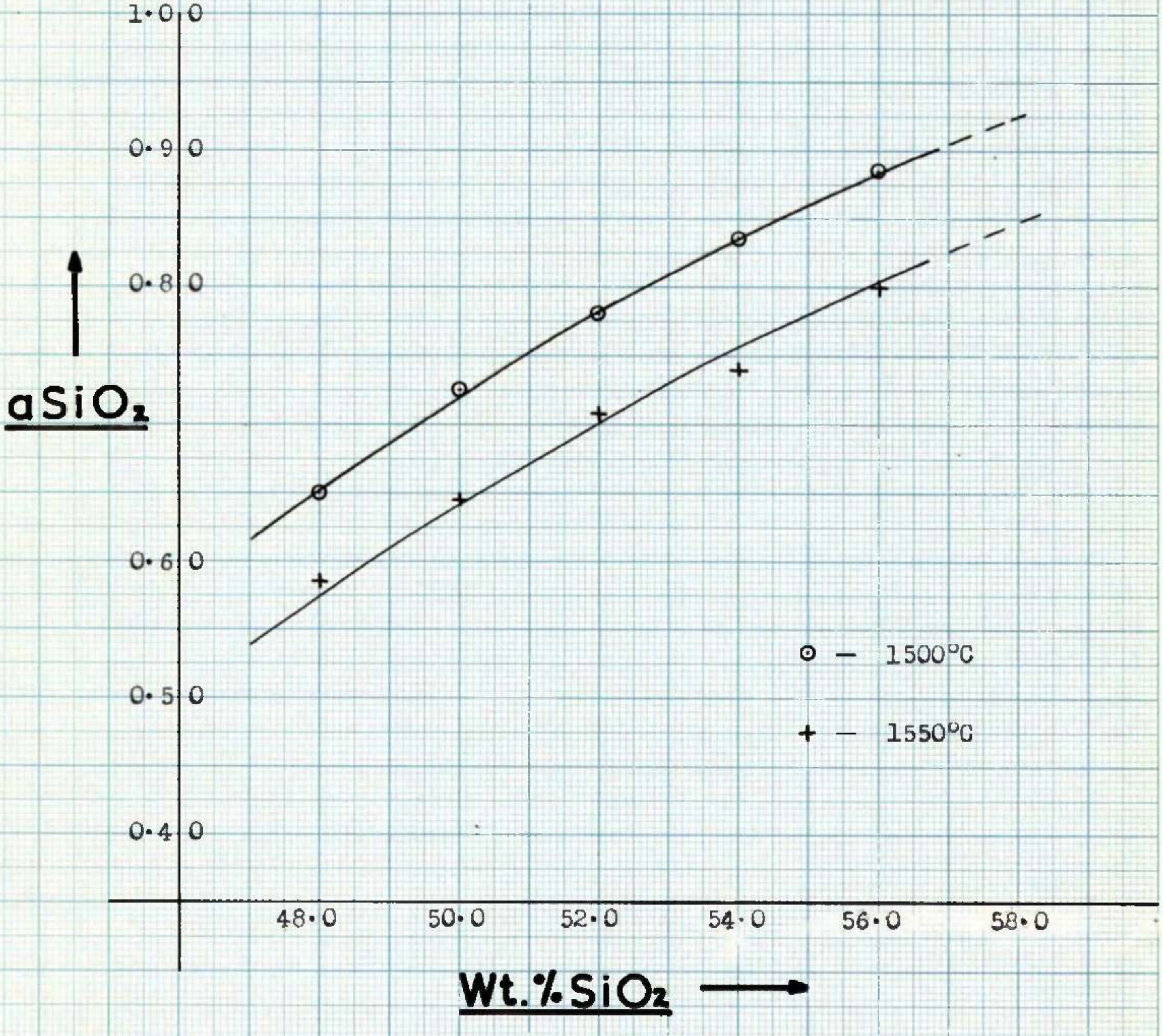

Silica activities of $MgO-Al_2O_3-SiO_2$ slags

(30% Al_2O_3)

FIG. 15

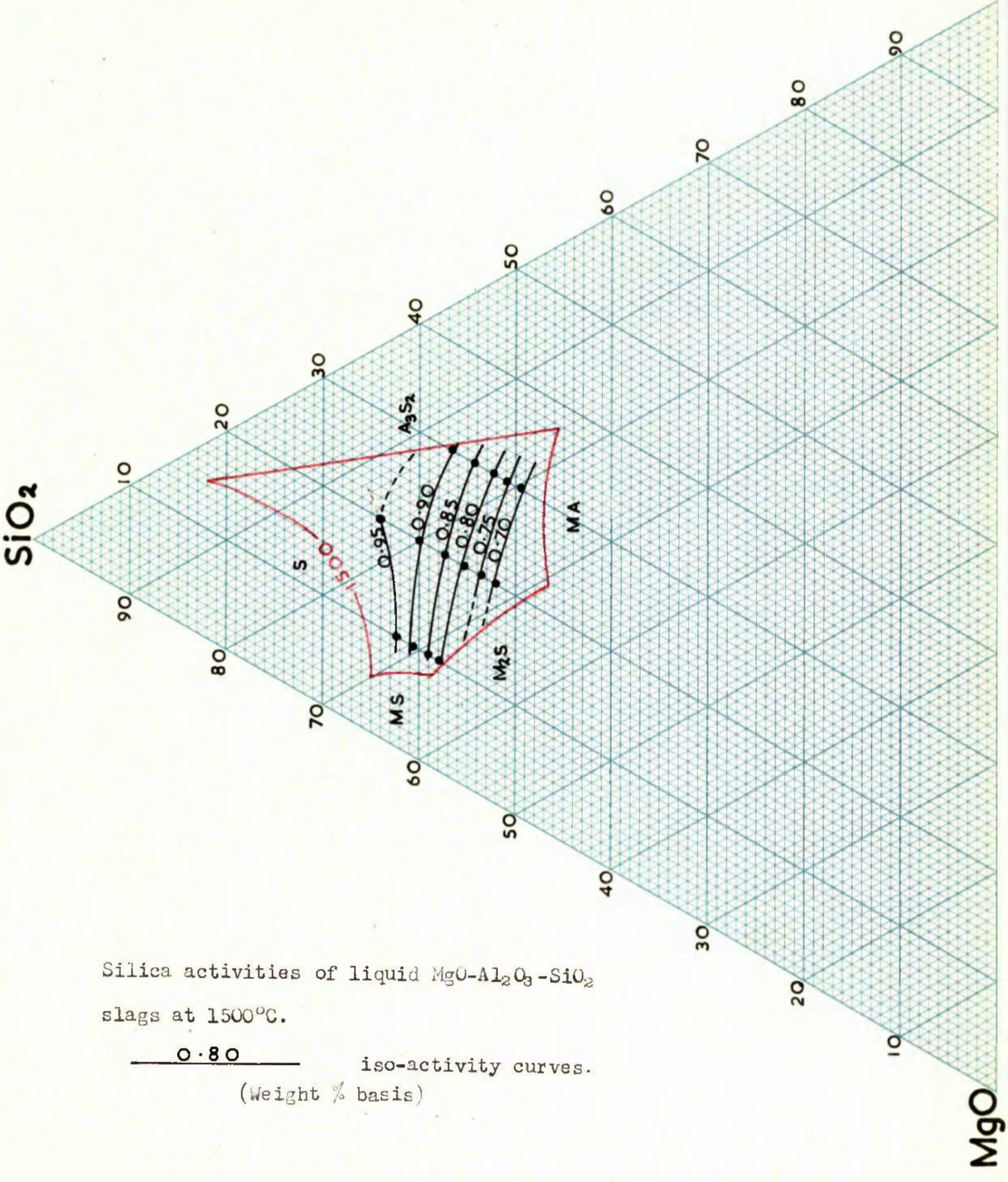

Silica activities of liquid $MgO-Al_2O_3-SiO_2$ slags at 1500°C.

0·80 ——— iso-activity curves.

(Weight % basis)

FIG.16

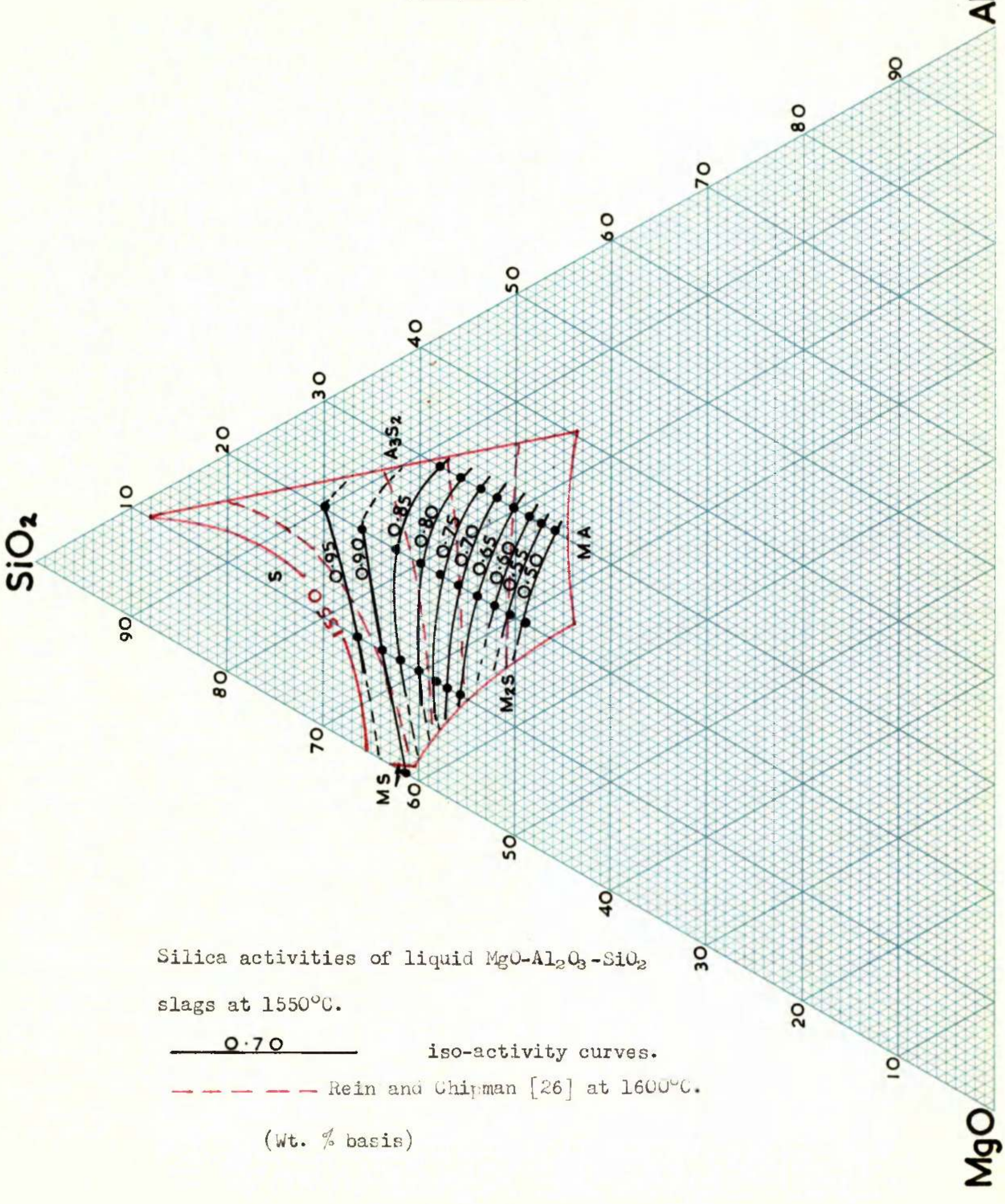

Silica activities of liquid $MgO-Al_2O_3-SiO_2$ slags at 1550°C.

0·70 ——— iso-activity curves.

– – – – Rein and Chipman [26] at 1600°C.

(Wt. % basis)

CHAPTER IV

DISCUSSION OF RESULTS

DISCUSSION OF RESULTS

THE CaO-MgO-SiO_2 SYSTEM

Comparison with Rein and Chipman [26]

Rein and Chipman have investigated the CaO-MgO-SiO_2 system by equilibrating liquid slags with liquid Fe-Si-C alloys in graphite crucibles at 1600°C in CO gas according to the equation

$$SiO_2(\text{slag}) + 2C(\text{gr.}) = \underline{Si}\ (\text{in Fe}) + 2CO(g) \quad \ldots \quad (10)$$

With carbon monoxide gas at 1 atmosphere the equilibrium constant in this reaction reduces to $K_{10} = a_{Si}/a_{SiO_2}$. This equilibrium constant K_{10} can be obtained from the free energy data for silica and carbon monoxide. The data obtained by Rein and Chipman were presented in the form of lines of constant silicon content in the metal which are also lines of constant silica activity in the slag. In order to convert these values of constant silicon content to values of silica activities, the thermodynamic data relating to silicon in iron solution are required.

There are two sets of experimental data available which can be used for this conversion. These are in close agreement with each other.

Baschwitz and Chipman [27] have investigated the distribution of silicon between liquid iron and iron-carbon alloys and liquid silver and obtained values of activities of silicon in iron-carbon alloys by use of activities of silicon in silver. The activities of silicon in silver were obtained from the silicon-silver phase diagram recently redetermined by Hager [28]. The use of this diagram involves an arbitrary correction in the data as given by Hager.

Smith and Taylor [29] also investigated the distribution of silicon between liquid iron and iron-carbon alloys and liquid silver but in order to obtain the activities of silicon in iron-carbon alloys from these data, a study was also made of the solubility of silicon in liquid silver in equilibrium with silicon carbide. The activities of silicon in silver were now obtained using the free energy of formation of silicon carbide given by Kay and Taylor [5]. These activities were then used to obtain activities of silicon in iron-carbon alloys.

In the first set of data the silicon distribution measurements are used in conjunction with activities of silicon in silver obtained from the silicon-silver phase diagram. These activities can be used to determine the free energy of formation of silicon carbide.

Alternatively, as in the second set of data, the free energy of formation of silicon carbide is used to obtain activities of silicon in silver. The difference in the value obtained for the free energy of formation of silicon carbide from the phase diagram and that determined by Kay and Taylor is only 750 cals.

As the present investigation involves the reaction

$$SiO_2(\overset{\beta}{\text{crist.}}) + 3C(gr) = SiC(cub.) + 2CO(g) \qquad .... (3)$$

from which Kay and Taylor obtained the free energy of formation of silicon carbide, it was decided to use the second set of data (Smith and Taylor) to get a comparison between the results obtained in the present work and those determined by Rein and Chipman. This means that the use of data is consistent in both cases.

An examination of the data produced by Rein and Chipman shows that, although they have drawn lines of constant silicon content in the metal over the range 40 - 70% by weight of silica, their experimental values only cover the range 43 - 49% silica. The other values have been obtained by extrapolation. Within the experimental range lie three lines of constant silicon content in the metal, i.e. 16%, 22% and 23% silicon by weight. These were converted to lines of constant silica activity in the slag (using the data determined by Smith and Taylor) to give silica activities of 0·061, 0·217 and 0·275 respectively.

The above results are compared with those produced in the present work at 1550°C in Figure 10. As can be seen the agreement is not good.

Iso-silica Activity Lines

The results of the present investigation are presented as iso-activity lines of silica in the liquid region of the $CaO-MgO-SiO_2$ system at 1500 and 1550°C. In Figure 23 (1550°C) the results are shown on a mole fraction basis. Examination of these results at high silica content shows a drop in silica activity along a line of constant silica content as magnesia is replaced by lime. At lower silica content the iso-activity lines change their shape and start to curve upwards as they approach the liquidus surface on the magnesia side of the ternary system. A comparison of the results obtained at 1500 and 1550°C (Figures 9 and 10) shows that as the liquidus surface retreats the iso-activity lines tend to straighten out. In other words, the shape of the iso activity lines from silica activity of 0·9 to 0·6 shows the true tendency due to the relative effects of magnesia and lime on the silica activity. This tendency would continue at lower silica contents but for the presence of the liquidus surface which distorts the curves upwards.

An examination of the binary eutectic trough between forsterite solid solution and magnesia in the equilibrium phase diagram of the CaO-MgO-SiO$_2$ system (Figure 5) can give comparative values of silica activities at 1500, 1550 and 1600°C. Along this trough the following reaction holds

$$M_2S \;=\; 2MgO + SiO_2 \quad \ldots\ldots\ldots\ldots\ldots \quad (11)$$

[Note : In the above equation $M_2S = 2MgO.SiO_2$, i.e. $M = MgO$ $S = SiO_2$. This procedure will be continued and include $C = CaO$ and $A = Al_2O_3$]. Now within the considered temperature range 1500 - 1600°C, the liquid slag is saturated with pure magnesia and forsterite solid solution, therefore $a_{MgO} = 1$ and $a_{M_2S} < 1$. Thus the equilibrium constant of reaction (11) $K_{11} = a_{SiO_2}/a_{M_2S}$. The free energy of forsterite can now be used to obtain the following equation

$$\log a_{SiO_2} \;=\; \frac{\Delta G^{\circ}_{M_2S}}{4\cdot 575\ T} \;+\; \log a_{M_2S} \quad \ldots . \quad (12)$$

As the temperature increases from 1500 - 1600°C the term $\dfrac{\Delta G^{\circ}_{M_2S}}{4\cdot 575\ T}$

will decrease, and due to solid solution decreasing, the activity of forsterite will increase and log a_{M_2S} will decrease. Thus an increase in temperature from 1500 - 1600°C gives a decrease in log a_{SiO_2} and an increase in the activity of silica.

The points on the binary eutectic trough between magnesia forsterite solid solution at 1500, 1550 and 1600°C all lie on a line of nearly constant silica content and an increase of silica activity with increasing temperature appears to be at variance with the data produced in the present investigation. The probable explanation is that (as mentioned previously) the shape of the curves at these low silica contents changes as the temperature increases and the liquidus surface retreats. This change is considered sufficient to produce the above effect.

Correlation of the Present Results with Free Energies of Formation of Interoxide Compounds

It was decided that it would be desirable to make use of the thermodynamic data, given by Kelley [30], of certain of the interoxide compounds found in the $CaO-MgO-SiO_2$ system as a cross check of the present results. It was thought that these data might also be used to amend the present results, if necessary, and extend them a certain amount.

With this end in view, silica activities were obtained from the free energies of formation of interoxide compounds and reactions at certain saturation troughs in the equilibrium phase diagram. It was found that the silica activities so obtained were not consistent with the activities determined experimentally. This led to an examination of the free energy data given by Kelley and it was found that certain of these data were incompatible with each other as will be shown later.

This means that some of Kelley's data are unreliable and thus cannot be used as a cross check of the present results as first considered.

It was now decided to use the present experimental results and from these data obtain estimates of the free energies of formation of some of the interoxide compounds found in the $CaO-MgO-SiO_2$ system. The reliability of the $CaO-MgO-SiO_2$ equilibrium phase diagram now becomes very important.

The Free Energies of Formation of Forsterite (M_2S) and Clinoenstatite (MS)

At 60·8% silica by weight and 1557°C on the SiO_2-MgO binary (Figure 5), a peritectic reaction takes place. The liquid slag is saturated with respect to both forsterite and clinoenstatite and this can be represented by the following equation

$$2MS = M_2S + SiO_2 \qquad \ldots\ldots\ldots \qquad (13)$$

As both forsterite and clinoenstatite are in their standard states, the equilibrium constant reduces to $K_{13} = a\ SiO_2$. The free energies of formation of forsterite and clinoenstatite at 1557 °C can be obtained from Kelley [30] and used to determine the free energy change of the above reaction (13).

$$\text{i.e.} \qquad \Delta G^{\circ}_{13} = \Delta G^{\circ}_{M_2S} - 2\Delta G^{\circ}_{MS}$$

$$\text{thus} \qquad \Delta G^{\circ}_{13} = -500 \text{ cal./mol.}$$

The free energy of formation of reaction (1^3) can also be obtained from the equation

$$\Delta G^{\circ}_{13} = -RT \ln K$$

$$\therefore \quad -500 = -4{\cdot}575 \times 1830 \times \log a_{SiO_2}$$

$$\therefore \quad a_{SiO_2} = 1{\cdot}15$$

This is, of course, impossible and means that either the free energy of formation of forsterite or of clinoenstatite is wrong, or that both are wrong.

It is possible to obtain the activity of silica at 60·8% silica on the SiO_2-MgO binary at 1550°C from Figure 10. This gives $a_{SiO_2} = 0{\cdot}9$ and this can be used to obtain the following relationship between the free energies of formation of forsterite and clinoenstatite from equation (13).

$$\text{i.e.} \quad \Delta G^{\circ}_{13} = \Delta G^{\circ}_{M_2S} - 2\Delta G^{\circ}_{MS}$$

$$\therefore \quad \Delta G^{\circ}_{M_2S} - 2\Delta G^{\circ}_{MS} = -4{\cdot}575 \times 1830 \times \log 0{\cdot}9$$

$$\text{thus} \quad \Delta G^{\circ}_{M_2S} - 2\Delta G^{\circ}_{MS} = 400 \text{ cal./mol.}$$

The activity of silica on the binary eutectic trough between forsterite solid solution and magnesia at 1550°C (i.e. CaO=29·0, MgO= 29·8 and SiO_2 = 41·2) is obtained from Figure 8. This is given as $a_{SiO_2} = 0{\cdot}065$. Along this trough the following reaction holds

$$M_2S = 2MgO + SiO_2 \quad \ldots\ldots\ldots \quad (11)$$

and as the slag is saturated with pure magnesia, $a_{MgO} = 1$. Assuming for the moment that forsterite is pure, then the equilibrium constant for reaction (11) reduces to $K_{11} = a_{SiO_2}$. This means that the free energy of formation of forsterite is given by

$$\Delta G^{\circ}_{M_2S} = 4{\cdot}575 \times 1823 \times \log 0{\cdot}065$$

$$= -\ 9{,}900 \text{ cal./mol.}$$

This value of - 9,900 cal./mol is a maximum value because forsterite is in solid solution and its activity is therefore less than 1.

$$\text{i.e. } \Delta G^{\circ}_{M_2S} = -\ 9{,}900 - 8{,}335 \log a_{M_2S}$$

For reasons which will be explained later in the discussion it was decided to make a tentative estimate of the free energy of formation of forsterite at 1550°C as - 9,000 cal./mol. Now from the relationship between forsterite and clinoenstatite which has just been derived

$$-\ 9{,}000 - 2\,\Delta G^{\circ}_{MS} = 400$$

$$\therefore\ \underline{\Delta G^{\circ}_{MS} = -\ 4{,}700 \text{ cal./mol}}$$

The values at 1550°C given by Kelley are

$$\underline{\Delta G^{\circ}_{M_2S} = -\ 15{,}100 \text{ cal./mol.}}$$

$$\text{and} \qquad \underline{\Delta G^{\circ}_{MS} = -\ 7{,}350 \text{ cal./mol}}$$

The Free Energy of Formation of Merwinite (C_3MS_2)

At 1575°C ($CaO = 43\cdot0$, $MgO = 18\cdot2$, $SiO_2 = 38\cdot8$) the liquid slag is saturated with respect to merwinite, calcium orthosilicate and magnesia and a peritectic reaction takes place (Figure 5). This can be represented by the equation

$$2C_3MS_2 \quad = \quad 3C_2S \; + \; 2MgO \; + \; SiO_2 \qquad \ldots\ldots \quad (14)$$

Merwinite, calcium orthosilicate and magnesia are all in their standard states, therefore the equilibrium constant for reaction (14) reduces to $K_{14} = a_{SiO_2}$. From Figure 10 the activity of silica at 1550°C at the point in question = 0·06, and this value is taken as the activity of silica at 1575°C. It is considered that this is within the experimental accuracy at this point. Using this value of the silica activity, the free energy change for reaction (14) is obtained

$$\Delta G^\circ_{14} \quad = \; - \, 4\cdot575 \; x \; 1848 \; x \; \log 0\cdot06$$

$$\text{i.e. } \Delta G^\circ_{14} \quad = \quad 10{,}300 \text{ cal/mol}$$

Now the free energy of formation of calcium orthosilicate has been firmly established [31, 32, 33], therefore taking the value given by Kelley [30] and using the free energy change for reaction (14) just derived, it is possible to obtain a value for the free energy of formation of merwinite at 1550°C

$$\text{i.e.} \quad \Delta G^{\circ}_{14} = 3\Delta G^{\circ}_{C_2S} - 2\Delta G^{\circ}_{C_3MS_2}$$

$$\therefore \quad 2\Delta G^{\circ}_{C_3MS_2} = -102{,}750 - 10{,}300$$

$$\therefore \quad \underline{\Delta G^{\circ}_{C_3MS_2} = -56{,}500 \text{ cal./mol}}$$

This can be compared with the value given by Kelley at this temperature

$$\text{i.e.} \ \underline{\Delta G^{\circ}_{C_3MS_2} = -55{,}250 \text{ cal./mol}}$$

The Free Energy of Formation of Monticellite (CMS)

At 1490°C ($CaO = 37{\cdot}4$, $MgO = 22{\cdot}4$, $SiO_2 = 40{\cdot}2$) the liquid slag is saturated with respect to monticellite, merwinite and magnesia and a peritectic reaction takes place (Figure 5). This can be represented by the equation

$$3\,CMS = C_3MS_2 + 2MgO + SiO_2 \qquad \text{......} \ (15)$$

Monticellite, merwinite and magnesia are all in their standard states therefore the equilibrium constant for reaction (15) reduces to $K_{15} = a\,SiO_2$. From Figure 9 the activity of silica at 1500°C at this point = 0·1. It is considered that it is within experimental accuracy to use this value at 1490°C. Thus the free energy change for reaction (15) is given by

$$\Delta G^\circ_{15} = -4{\cdot}575 \times 1763 \times \log 0{\cdot}1$$

i.e. $\Delta G^\circ_{15} = 8{,}100$ cal./mol.

Now using this value for the free energy change for reaction (15) and the value just obtained for the free energy of formation of merwinite, corrected for the temperature difference using Kelley's temperature coefficient, it is possible to obtain a value for the free energy of formation of monticellite at 1490°C

i.e. $\Delta G^\circ_{15} = \Delta G^\circ_{C_3MS_2} - 3\Delta G^\circ_{CMS}$

$\therefore\ 3\Delta G^\circ_{CMS} = -56{,}400 - 8{,}100$

$\therefore\ \underline{\Delta G^\circ_{CMS} = -21{,}500 \text{ cal./mol.}}$

It can be seen that this does not agree well with the value given by Kelley at this temperature

i.e. $\underline{\Delta G^\circ_{CMS} = -26{,}800 \text{ cal./mol.}}$

In order to determine which of the above values for the free energy of formation of monticellite is the more reliable, Kelley's data for both the free energies of formation of merwinite and monticellite were used to obtain the free energy change for the following reaction at 1490°C

$$3\ CMS = C_3MS_2 + 2MgO + SiO_2 \quad \ldots\ldots \quad (15)$$

From this one can obtain the activity of silica at the point where the peritectic reaction takes place. This gave the ridiculous value of $aSiO_2 < 10^{-3}$ and shows that something is wrong with the thermodynamic data given by Kelley. It will be shown later in the discussion that the value given by Kelley for the free energy of formation of monticellite is incompatible with other interoxide data also given by Kelley and an examination of these data strongly suggests that the free energy of formation of monticellite as given by Kelley is unreliable.

Application of the Gibbs-Duhem Relationship to the Ternary System CaO-MgO-SiO_2. i.e. Schumann's Method

The Gibbs-Duhem relationship can be extended to evaluate the activities of the other two components in a ternary system when the activities are known for one component over a range of compositions.

Schumann has proposed a method of evaluation whereby the activities of two components, in this case lime and magnesia, can be derived by drawing tangents from lines of constant activity for the third component, silica, to intercept either the silica-lime or the silica-magnesia side of the ternary system.

Taking magnesia as an example, a line of constant molar ratio N_{MgO}/N_{CaO} is drawn from pure silica to meet any convenient point in the system where the activity of magnesia is known. This line cuts the lines of constant silica activity at certain points and tangents are drawn from these points to intercept the silica-magnesia side of the ternary. Magnesia activities are obtained from the equation.

$$\ln aMgO\ (m) = \left[\ln a\ MgO\ (n) - \int_{aSiO_2(n)}^{aSiO_2(m)} \left(\frac{NSiO_2}{NMgO} \right)_{aSiO_2 . aCaO} \cdot d \ln aSiO_2 \right]_{\frac{NMgO}{NCaO}}$$

where m and n are the limits of the integration paths along the line of constant molar ratio N_{MgO}/N_{CaO}. The values of the binary intercepts, corresponding to $\left(\frac{NSiO_2}{NMgO} \right)_{a_{SiO_2} \cdot a_{CaO}}$ are plotted against ln a SiO_2 and the integral is equal to the area under the curve between the limits ln $a_{SiO_2}(m)$ and ln a_{SiO_2} (n).

Magnesia Activities at 1550°C

Two convenient starting points were first of all chosen. These are both points of magnesia saturation and therefore $a_{MgO} = 1$ in both cases. The points are (CaO = 29·0, MgO = 29·8, SiO_2 = 41·2) and (CaO = 40·8, MgO = 20·0, SiO_2 = 39·2) and the activities of silica at these points were obtained by a small extrapolation as shown in Figures 6 and 7 as 0·065 and 0·08 respectively. Magnesia activities were obtained from Figure 10 by the Gibbs-Schumann method as explained and the values are shown in Figure 18. The values of the binary intercepts and of ln a_{MgO} obtained from the areas under curves are shown in Tables D and E in the appendix.

Lime Activities at 1550°C

Again two convenient starting points were chosen. In this case they are both points of calcium orthosilicate saturation i.e. $a_{C_2S} = 1$. Accepting that the free energy of formation of calcium orthosilicate is firmly established it is possible to obtain the activities of lime at these points using the equation

$$C_2S = 2\,CaO + SiO_2 \qquad \text{..........} \quad (16)$$

The equilibrium constant for reaction (16) reduces to $K_{16} = a^2_{CaO} . a_{SiO_2}$. The points are (CaO = 48·6, MgO = 10·0, SiO_2 = 41·4) and (CaO = 41·5, MgO = 19·0, SiO_2 = 39·5) and the silica activities at these points were obtained from Figures 6 and 7 as both equal to 0·08. Using the free energy of formation of calcium orthosilicate given by Kelley at 1550°C then

$$\Delta G^{\circ}_{C_2S} = + 4{\cdot}575 \times 1823 \times \log (a^{2}_{CaO} \cdot 0{\cdot}08)$$

$$\text{i.e. } a_{CaO} = 0{\cdot}032$$

It is now possible to obtain lime activities along lines of constant molar ratio N_{MgO}/N_{CaO} by the Gibbs-Schumann method.

The lime activities obtained are shown in Figure 20 and the working data are shown in Tables I and J in the appendix.

Magnesia Activities at 1500°C

In this case it is not possible to obtain convenient starting points on the magnesia saturation line which are on, or are very close to, the 20% or 30% magnesia lines. As can be seen from Figure 5, the activities of silica at 1500°C along the 30% magnesia line are limited by the liquidus surface. A starting point for the Gibbs-Schumann integration was chosen at ($CaO = 32{\cdot}5$, $MgO = 26{\cdot}2$, $SiO_2 = 41{\cdot}3$) which is the highest value of magnesia that can be obtained on the line of magnesia saturation. It is now necessary to have the activity of silica at this point. As this point does not lie on, or very close to, either the 20% or 30% magnesia lines it is not possible to obtain this silica activity from either Figures 7 or 8. To obtain it from the iso-silica activity lines at 1500°C (Figure 9) involves a rather dubious extrapolation, because of the distortion of the iso-silica lines as they approach the liquidus surface.

In fact, this extrapolation was carried out and a value of silica activity = 0·1 was obtained. It was decided to test this value by using it to determine the free energy of formation of forsterite at 1500°C from the binary eutectic trough between forsterite solid solution and magnesia and comparing it with that previously determined at 1550°C. This can be represented by the equation

$$M_2S \quad = \quad 2MgO + SiO_2 \qquad \ldots\ldots \qquad (11)$$

Assuming pure forsterite, the equilibrium constant for reaction (11) reduces to $K_{11} = a_{SiO_2}$ and the free energy of formation of forsterite at 1500°C is given by

$$\Delta G^\circ_{M_2S} \quad = \quad + \; 4{\cdot}575 \times 1773 \times \log 0{\cdot}1$$

$$\text{i.e. } \underline{\Delta G^\circ_{M_2S} \quad = \quad - \; 8{,}100 \text{ cal./mol.}}$$

This can now be compared with the value obtained at 1550°C

$$\text{i.e. } \underline{\Delta G^\circ_{M_2S} \quad = \quad - \; 9{,}900 \text{ cal./mol.}}$$

These values are both maximum values because forsterite is in solid solution. There will be more solid solution at 1500°C than at 1550°C, therefore the 'true' values will show a difference over 50°C of more than 1,800 cal./mol. It is usually found that errors in free energy data can be traced to errors in the enthalpy data and that heat capacity data which are used to obtain the entropy term are fairly reliable. It was therefore assumed that the temperature coefficient for the free energy of forsterite given by Kelley is approximately correct, although the actual values have been shown to be wrong, then the free energy of formation of forsterite would alter by less than 100 cal. over 50°C. Thus it is likely that the silica activity obtained by the extrapolation at 1500°C is wrong.

A value for the silica activity at 1500°C can be obtained by assuming that the amount of solid solution of forsterite will increase only slightly as the temperature falls from 1550° - 1500°C. Thus the free energy of formation of forsterite solid solution at 1500°C will be only slightly smaller than - 9,900 cal./mol. and this value can be used to estimate the silica activity at 1500°C. A value of silica activity at 1500°C of 0·065 is given for this point, i.e. ($CaO = 32 \cdot 5$, $MgO = 26 \cdot 2$, $SiO_2 = 41 \cdot 3$).

It is now possible to draw an iso-silica activity line of 0·065 by obtaining points on the 10% and 20% magnesia lines by extrapolation. The Gibbs-Schumann integration was now carried out and the magnesia activities obtained are shown in Figure 17. The working data are shown in Table A in the appendix.

A second starting point for Gibbs-Schumann integration was chosen at (CaO = 37·5, MgO = 22·3, SiO_2 = 40·2). This is the lowest value of magnesia that can be obtained on the magnesia saturation line at 1500°C. This means that the iso-magnesia lines obtained cover the widest possible range of compositions. It was now necessary to obtain the activity of silica at this point and this was determined from the shape of the iso-activity lines of silica at 1500°C (Figure 9) and the activity of silica on the 20% magnesia line at 40% silica (Figure 7). This gives a value of silica activity of 0·1.

As before the Gibbs-Schumann integration was carried out and the magnesia activities obtained are shown in Figure 17. The working data are shown in Table B in the appendix.

Extension of Magnesia Activities at 1500°C

The CaO-MgO-SiO_2 system was examined with a view to extending the magnesia activities over as wide a composition range as possible.

At the point ($CaO = 47{\cdot}0$, $MgO = 11{\cdot}3$, $SiO_2 = 41{\cdot}7$) on the binary eutectic trough between merwinite and calcium orthosilicate at 1500°C, the activity of silica is obtained from the shape of the iso-silica activity lines (Figure 9) and the activity of silica on the 10% magnesia line at 42% silica (Figure 6). This gives a silica activity of 0·135. At this point the liquid slag is saturated with merwinite and calcium orthosilicate and this can be represented by the equation

$$2\ C_3MS_2 \quad = \quad 3C_2S \ + \ 2MgO \ + \ SiO_2 \qquad \ldots\ldots\ldots \quad (14)$$

The equilibrium constant for reaction (14) reduces to $K_{14} = a^2_{MgO} \cdot a_{SiO_2}$. The free energy of formation of merwinite has been determined at 1575°C using the present data and in order to obtain magnesia activities which are consistent, this value was used in conjunction with the temperature coefficient given by Kelley to give the free energy of formation of merwinite at 1500°C.

$$\text{i.e. } \Delta G^\circ_{C_3MS_2} \quad = \quad -\ 56{,}700 \text{ cal./mol.}$$

The free energy of formation of calcium orthosilicate at 1500°C from Kelley is given as

$$\Delta G^\circ_{C_2S} \quad = \quad -\ 33{,}800 \text{ cal./mol}$$

Now the free energy change for reaction (14) is given by the equations

$$\Delta G^\circ_{14} = -4{\cdot}575 \times 1773 \times \log (a^2_{MgO} . 0{\cdot}135)$$

and $$\Delta G^\circ_{14} = 3\,\Delta G^\circ_{C_2S} - 2\,\Delta G^\circ_{C_3MS_2}$$

Therefore the activity of magnesia at this point is obtained as 0·49.

The Gibbs-Schumann integration was now carried out and the magnesia activities are shown in Figure 17 joined the other activities by broken lines to indicate that the other values given are more reliable. The working data are shown in Table C in the appendix.

The iso-magnesia activity lines can also be extended at 1500°C to meet the forsterite saturation line. This can be represented by the equation

$$M_2S = 2MgO + SiO_2 \quad ....(11)$$

where the equilibrium constant reduces to $K_{11} = a^2_{MgO} \cdot a_{SiO_2}$. It has been estimated previously from the present data that the free energy of formation of forsterite at 1550°C is -9,000 cal./mol. The temperature coefficient given by Kelley is small therefore this figure of - 9,000 cal./mol. was also taken by 1500°C. Now the free energy of formation of forsterite at 1500°C is also given by

$$\Delta G^{\circ}_{M_2S} = + 4{\cdot}575 \times 1773 \times \log (a^2_{MgO} . a_{SiO_2})$$

and if the silica activity is known then magnesia activity can be calculated.

Three points on the forsterite saturation line at 1500°C were now selected and the activities of silica were obtained at these points from Figure 9.

At point ($CaO = 11{\cdot}0$, $MgO = 31{\cdot}4$, $SiO_2 = 57{\cdot}6$) the silica activity is 0·8 and this gives <u>$a_{MgO} = 0{\cdot}31$</u>

At point ($CaO = 13{\cdot}0$, $MgO = 31{\cdot}0$, $SiO_2 = 56{\cdot}0$) the silica activity is 0·7 and this gives <u>$a_{MgO} = 0{\cdot}33$</u>.

At point ($CaO = 24{\cdot}0$, $MgO = 28{\cdot}4$, $SiO_2 = 47{\cdot}6$) the silica activity is 0·3 and this gives <u>$a_{MgO} = 0{\cdot}51$</u>

This last value is actually a maximum value because at this point forsterite is in solid solution and thus the activity of forsterite is less than 1. The values obtained are shown in Figure 17 again joined to the others by broken lines.

Free Energy of Formation of Forsterite

The free energy of formation of forsterite cannot be determined from the equilibrium phase diagram using the present results because of solid solution. A maximum value of -9,900 cal./mol. was obtained at 1550°C from the present results but pure forsterite appears in a number of equations in this discussion and it was essential to have a value for the free energy of formation of this compound in its pure state.

In the previous section of this discussion magnesia activities were obtained at three points on the forsterite saturation line by making use of the free energy of formation of forsterite. As can be seen from Figure 17, a decrease in the negative free energy of formation of forsterite below - 9,000 cal./mol would cause an increase in the values of magnesia activities along the forsterite saturation line causing the iso-magnesia activity lines to turn up even more sharply. Also the more the negative free energy of formation of forsterite is decreased from the maximum value of - 9,900 cal/mol. obtained from the present results, the further away it becomes from the value given by Kelley.

For these reasons a tentative figure of - 9,000 cal./mol. at 1550°C is placed on the free energy of formation of forsterite. It is realised that this only a tentative value but the free energy of formation of forsterite is necessary for a number of calculations carried out in this discussion and it is considered worth while to carry out the calculations using this tentative value because when a more reliable value is obtained for the free energy of formation of forsterite it will be a simple matter to amend these calculations.

Extension of Magnesia Activities at 1550°C

The magnesia activities can also be extended to meet the forsterite saturation line at 1550°C. As before

$$M_2S = 2MgO + SiO_2 \quad \ldots\ldots \quad (11)$$

where the equilibrium constant $K_{11} = a^2MgO.aSiO_2$ and the free energy of formation of forsterite at 1550°C is given by

$$\Delta G^{\circ}_{M_2S} = + 4{\cdot}575 \times 1823 \times \log (a^2MgO.aSiO_2)$$

As before, three points on the forsterite saturation line at 1550°C were selected and silica activities obtained from Figure 10.

At point ($CaO = 6{\cdot}0$, $MgO = 37{\cdot}0$, $SiO_2 = 57{\cdot}0$) the silica activity is 0·7 and this gives $\underline{aMgO = 0{\cdot}35}$

At point ($CaO = 11{\cdot}0$, $MgO = 35{\cdot}0$, $SiO_2 = 54{\cdot}0$) the silica activity is 0·5 and this gives $\underline{aMgO = 0{\cdot}41}$

At point ($CaO = 14{\cdot}0$, $MgO = 34{\cdot}0$, $SiO_2 = 52{\cdot}0$) the silica activity is 0·3 and this gives $\underline{aMgO = 0{\cdot}53}$

Again this last value is a maximum value due to the solid solution of forsterite.

It is possible to obtain the magnesia activity on the binary eutectic trough between merwinite and calcium orthosilicate at 1550°C in the same manner as this was obtained at 1500°C but examination of the equilibrium phase diagram (Figure 5) shows that this does not extend the iso-magnesia activity lines by very much. It was decided that it was not worthwhile to carry out a Gibbs-Schumann integration from this point.

Thus as can be seen from Figures 17 and 18 the magnesia activities are more extensive at 1500°C than at 1550°C. It is considered that the experimental results are likely to be more accurate at 1550°C and as magnesia activities will be used later in the discussion to obtain free energies of formation of certain interoxide compounds, the 1550°C iso-magnesia activity lines have been extrapolated by careful comparison with those at 1500°C. These final curves gives the best values for magnesia activities in the $CaO-MgO-SiO_2$ system and are shown in Figure 18.

Lime Activities at 1500°C

A convenient starting point was chosen on the 10% magnesia line where it crosses the 1500°C liquidus, i.e. ($CaO = 47{\cdot}9$, $MgO = 10{\cdot}0$, $SiO_2 = 42{\cdot}1$). At this point the liquid slag is saturated with calcium orthosilicate and thus $a_{C_2S} = 1$. The activity of silica is taken from Figure 6 as 0·135 and using this value and the free energy of formation of calcium orthosilicate,

FIG. 17

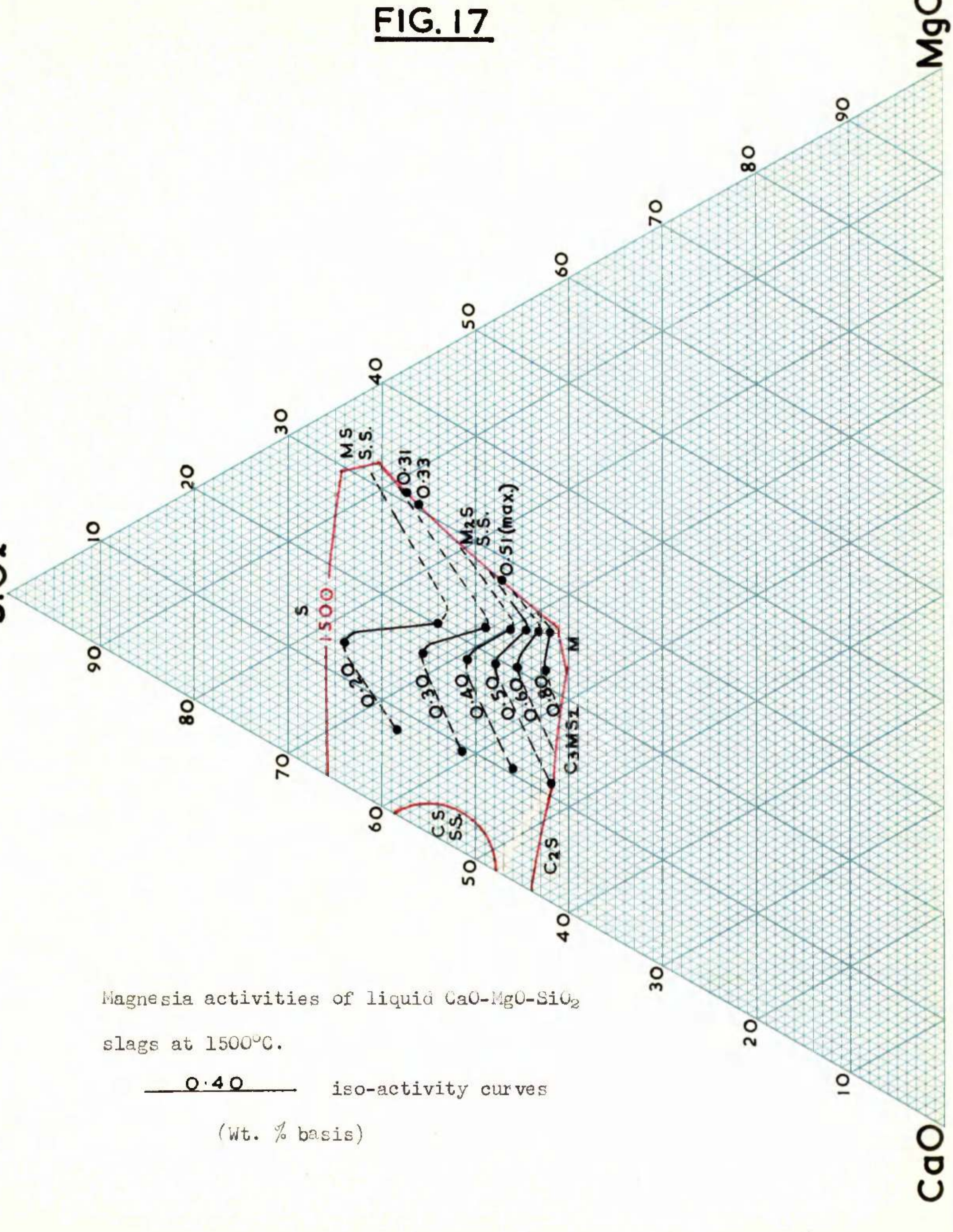

Magnesia activities of liquid CaO-MgO-SiO_2 slags at 1500°C.

0·40 ——— iso-activity curves

(Wt. % basis)

FIG. 18

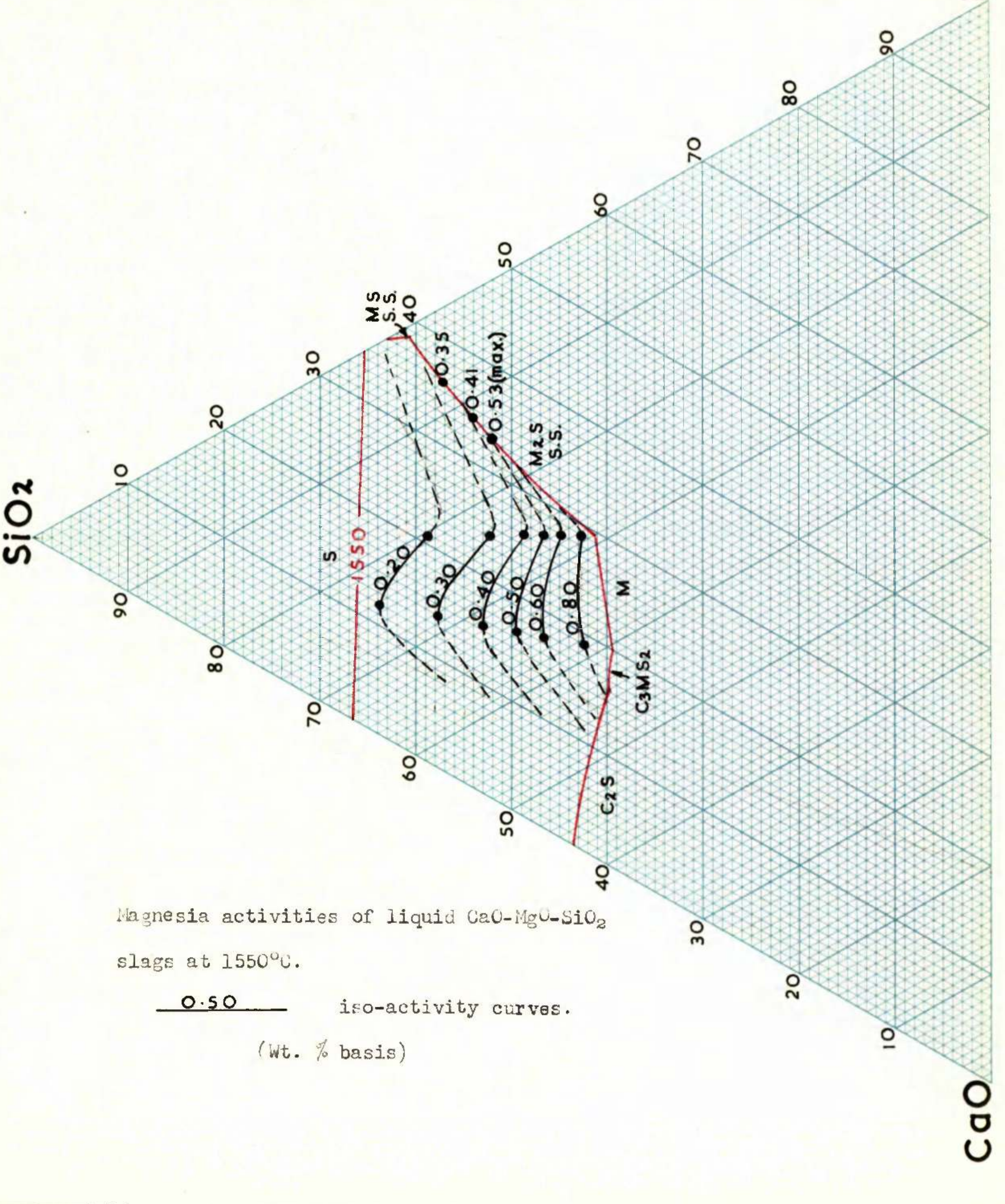

Magnesia activities of liquid $CaO-MgO-SiO_2$ slags at 1550°C.

0·50 — iso-activity curves.

(Wt. % basis)

the activity of lime at this point is calculated as 0·022. The lime activities were now calculated by the Gibbs-Schumann integration and are shown in Figure 19. The working data are shown in Table F in the appendix.

Another starting point for a Gibbs-Schumann integration was obtained by projecting the binary eutectic trough between calcium orthosilicate and magnesia until it cut the 1500°C liquidus. This occurred at (CaO = 39·3, MgO = 20·0, SiO_2 = 40·7). The silica activity was taken from Figure 7 as 0·115 and, as above, the activity of lime was calculated giving 0·024. Again the lime activities were calculated by the Gibbs-Schumann integration and are shown in Figure 19. The working data are shown in Table G in the appendix.

Extension of Lime Activities at 1500°C

The CaO-MgO-SiO_2 system was now examined with a view to extending the lime activities over as wide a composition range as possible.

At point (CaO = 32·5, MgO = 26·2, SiO_2 = 41·3) at 1502°C, the liquid slag is saturated with respect to monticellite, forsterite and magnesia and a peritectic reaction takes place. This can be represented by the equation

$$M_2S + CaO = CMS + MgO \quad \ldots\ldots\ldots \quad (17)$$

At this point forsterite is in solid solution and, as before, it is assumed that the amount of solid solution does not increase by very much as the temperature drops from 1550 - 1502°C. Thus the free energy of formation of forsterite solid solution at 1502°C is taken as that determined earlier in the discussion from the present results at 1550°C, i.e. - 9,900 cal./mol. The free energy of formation of monticellite is also taken as that determined earlier at 1490°C. Thus the free energy change for reaction (17) is given by the equations

$$\Delta G^\circ_{17} = \Delta G^\circ_{CMS} - \Delta G_{M_2S(\text{solid soln.})}$$

$$= -21{,}500 + 9{,}900$$

$$\text{also} \quad \Delta G^\circ_{17} = -4{\cdot}575 \times 1775 \times \log\left(\frac{1}{a_{CaO}}\right)$$

$$\therefore \quad a_{CaO} = 0{\cdot}037$$

The lime activities were now determined by use of the Gibbs-Schumann integration and are shown in Figure 19. The working data are shown in Table H in the appendix.

Also shown in Figure 19 are the lime activities along the $CaO-SiO_2$ binary calculated by use of the Gibbs-Duhem relationship from the silica activities obtained by Kay and Taylor [5] slightly modified as explained previously. These lime activities agree well with the results obtained by Carter and Macfarlane [2] who studied the equilibrium between the slags and the gas containing sulphur and determined a_{CaO} using the sulphur content in the slags.

Extension of Lime Activities at 1550°C

Lime activities at 1550°C also have been extended to the $CaO-SiO_2$ binary to meet the modified values obtained by Kay and Taylor from their silica activities by use of the Gibbs-Duhem relationship.

It is not possible to extend the lime activities towards the $MgO-SiO_2$ side of the ternary at 1550°C as was done at 1500°C but as in the case of magnesia activities, the lime activities at 1550°C were extrapolated by comparison with those at 1500°C as can be seen in Figure 20.

Comparison with Sawamura [34]

Sawamura has determined lime activities in the binary melt $CaO-SiO_2$ and in the ternary melt $CaO-MgO-SiO_2$ at 1600°C by e.m.f.

FIG. 19

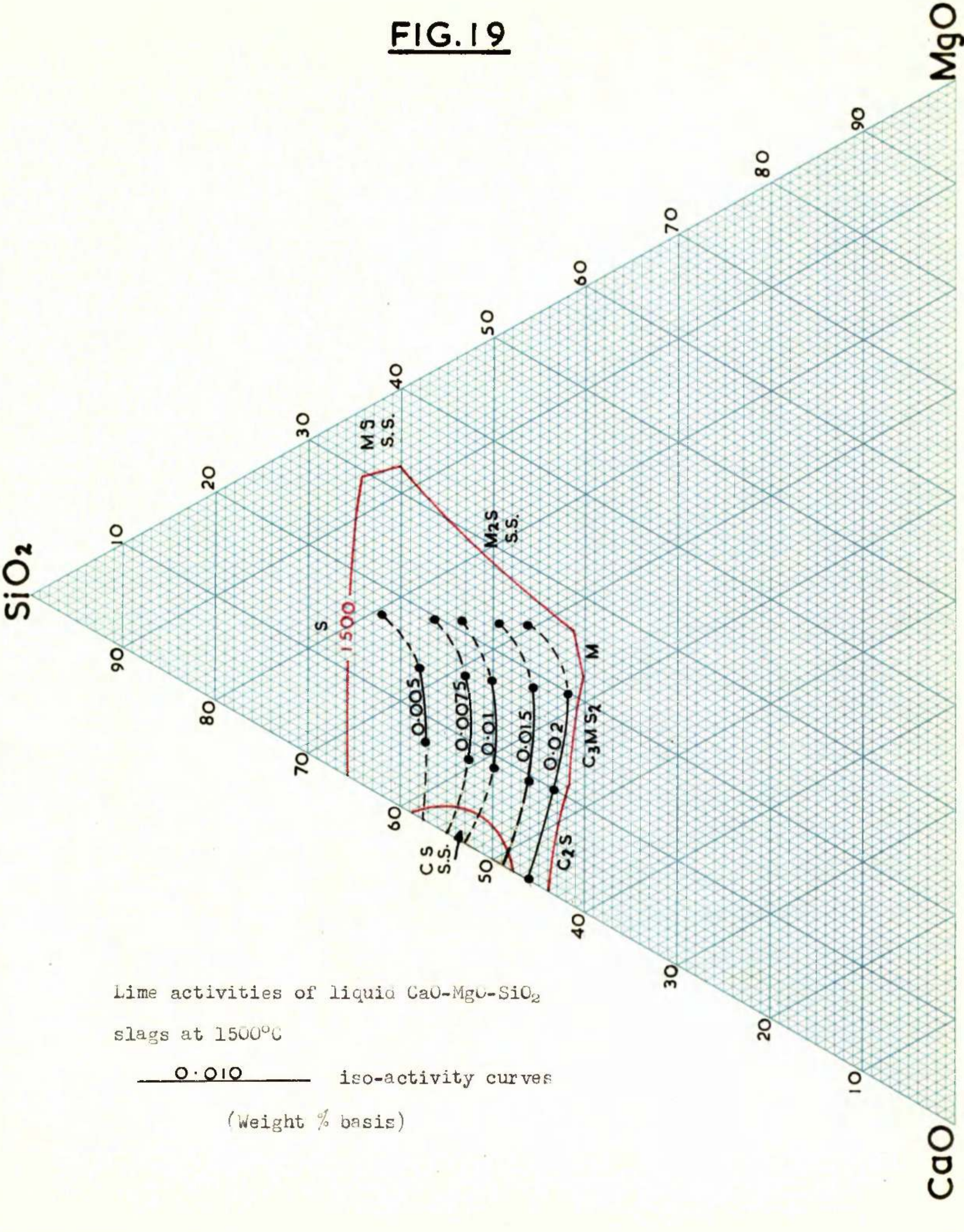

Lime activities of liquid CaO-MgO-SiO_2 slags at 1500°C

0·010 iso-activity curves

(Weight % basis)

FIG. 20

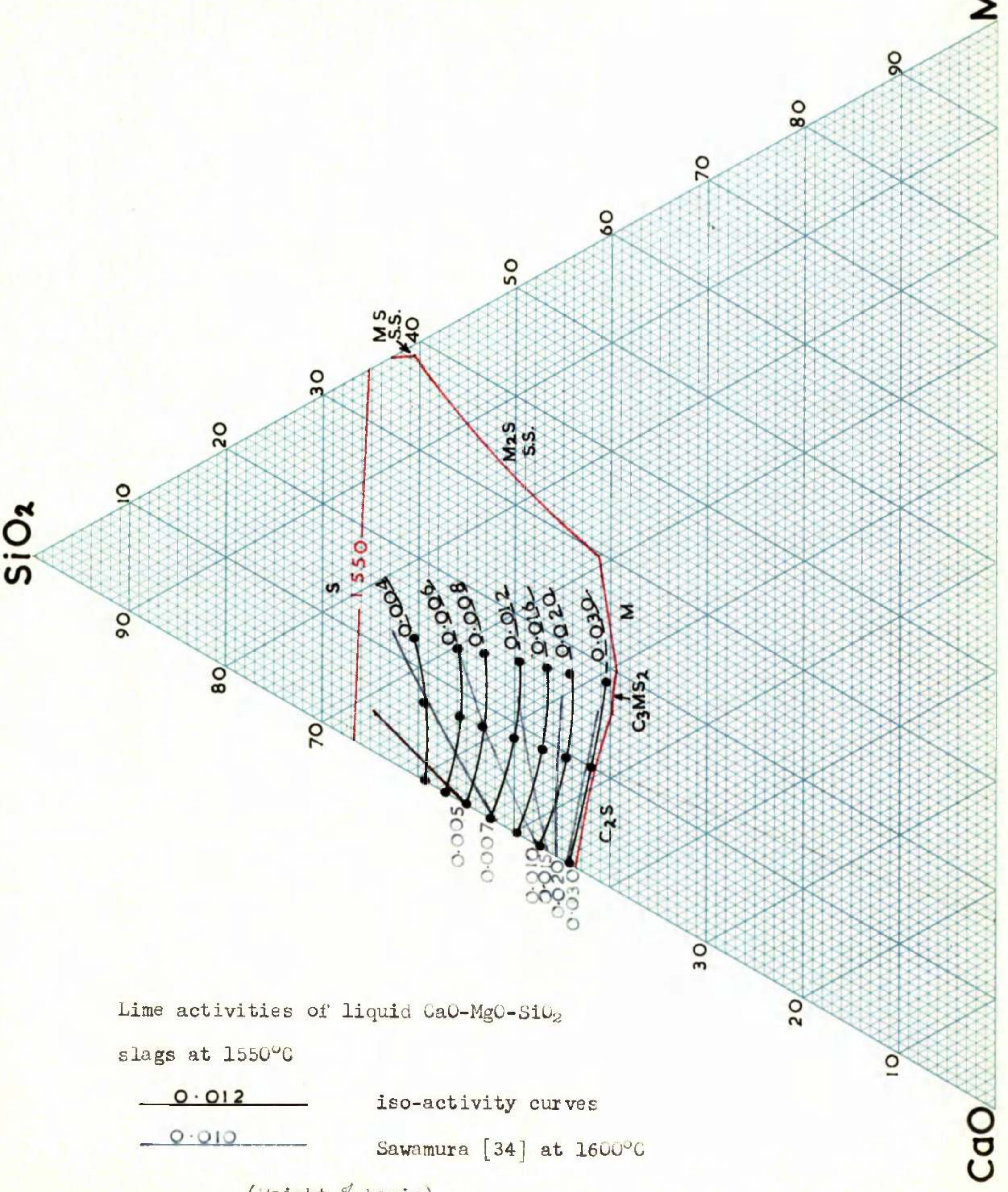

Lime activities of liquid CaO-MgO-SiO$_2$ slags at 1550°C

0·012 ——— iso-activity curves

0·010 ——— Sawamura [34] at 1600°C

(Weight % basis)

measurement of double cells. Sawamura's results are compared with the present results in Figure 20.

As can be seen the agreement is not good. Sawamura's results agree with neither the results obtained in the present investigation in the $CaO-MgO-SiO_2$ ternary melt nor with the results obtained by Kay and Taylor [5] in the $CaO-SiO_2$ binary melt which agree with a number of other investigators [2, 4, 6].

Free Energy of Formation of Diopside (CMS_2)

The free energy of formation of Diopside is given by the following equation

$$CaO + MgO + 2SiO_2 = CMS_2 \quad ..... \qquad (18)$$

and the equilibrium constant for reaction (18) is $K_{18} = \frac{1}{aCaO.aMgO.a^2SiO_2}$.

At 1550°C, the activities of silica, magnesia and lime were obtained at the diopside composition ($CaO = 25\cdot9$, $MgO = 18\cdot7$, $SiO_2 = 55\cdot4$) from Figures 10, 18 and 20 as (0·50, 0·3 and 0·007 respectively.

$$\therefore \Delta G^\circ_{CMS_2} = -4\cdot575 \times 1823 \times \log \frac{1}{(0\cdot007)(0\cdot3)(0\cdot50)^2}$$

hence $\underline{\Delta G^\circ_{CMS_2} = -28{,}000 \text{ cal./mol.}}$

From Kelley

$$\underline{\Delta G^\circ_{CMS_2} = -32{,}900 \text{ cal/mol.}}$$

Again the present results do not agree with Kelley.

Free Energy of formation of Akermanite (C_2MS_2)

The free energy of formation of Akermanite is given by the following equation

$$2CaO + MgO + 2SiO_2 = C_2MS_2 \quad \ldots\ldots \quad (19)$$

and the equilibrium constant for reaction (19) is $K_{19} = \dfrac{1}{a^2CaO.aMgO.a^2SiO_2}$.

At 1550°C, the activities of silica, magnesia and lime were obtained at the akermanite composition ($CaO = 41{\cdot}2$, $MgO = 14{\cdot}8$, $SiO_2 = 44{\cdot}0$) from Figures 10, 18 and 20 as 0·15, 0·6 and 0·023 respectively.

$$\therefore \quad \Delta G^\circ_{C_2MS_2} = -4{\cdot}575 \times 1823 \times \log \frac{1}{(0{\cdot}023)^2(0{\cdot}6)(0{\cdot}15)^2}$$

hence $\underline{\Delta G^\circ_{C_2MS_2} = -42{,}900 \text{ cal./mol.}}$

From Kelley

$\underline{\Delta G^\circ_{C_2MS_2} = -43{,}000 \text{ cal./mol.}}$ (an estimation at 1550°C

Thus in the above case a good agreement is found between the present results and the data given by Kelley.

Activities of Clinoenstatite obtained along the Clinoenstatite (MS)/ /Calcium Metasilicate (CS) join.

It is possible to obtain silica activities and magnesia activities at 1550°C at chosen points on the line joining the compounds clinoenstatite and calcium metasilicate from Figures 10 and 18.

respectively.

Using the equation

$$MgO + SiO_2 = MS \quad .... \qquad (20)$$

for which the equilibrium constant $K_{20} = \frac{a\,MS}{aMgO.aSiO_2}$, and the free energy of formation of clinoenstatite, it is possible to obtain the activities of clinoenstatite at certain points on the line joining the two metasilicates.

The question now arises as to which value should be used for the free energy of formation of clinoenstatite. The value given by Kelley at 1550°C is - 7,300 cal./mol. while the value obtained via the free energy of formation of forsterite from the present results is - 4,700 cal./mol. Kelley's value was used to obtain the activity of clinoenstatite at the composition of diopside (CMS_2) where the mole fraction of clinoenstatite is 0·5. This gave an activity of clinoenstatite which is greater than 1. This is additional evidence to point to the fact that the free energy of formation of clinoenstatite given by Kelley is unreliable.

Using the value obtained from the present work for the free energy of formation of clinoenstatite at 1550°C, clinoenstatite activities were obtained at three points on the line joining the metasilicates, i.e. at $N_{MS} = 0{\cdot}25$, $N_{MS} = 0{\cdot}5$ and $N_{MS} = 0{\cdot}75$.

At N_{MS} = 0·25 (CaO = 37·4, MgO = 9·0, SiO_2 = 53·6), the silica activity from Figure 10 is 0·4 and the magnesia activity from Figure 18 is 0·28

$$\therefore -4{,}700 = -4{\cdot}575 \times 1823 \times \log \frac{a_{MS}}{0{\cdot}4 \times 0{\cdot}28}$$

$$\text{i.e. } \underline{a_{MS} = 0{\cdot}41}$$

At N_{MS} = 0·5 (CaO = 25·9, MgO = 18·7, SiO_2 = 55·4), a_{SiO_2} = 0·50 from Figure 10 and a_{MgO} = 0·3 from Figure 18, hence $\underline{a_{MS} = 0{\cdot}54}$

At N_{MS} = 0·75 (CaO = 13·4, MgO = 29·0, SiO_2 = 57·6) a_{SiO_2} = 0·67 from Figure 10 and a_{MgO} = 0·25 from Figure 18, hence $\underline{a_{MS} = 0{\cdot}62}$.

Thus

N_{MS} = 0·25 , 0·5 , 0·75

a_{MS} = 0·41 , 0·54, 0·62

The above clinoenstatite activity values can be used to test the validity of the shape of the iso-magnesia activity lines. The iso-magnesia activity lines shown in Figure 18 are made up of two parts, i.e. the solid lines are magnesia activities obtained directly from the iso-silica activity lines by the Gibbs-Schumann integration, and the broken lines are magnesia activities obtained in a more indirect manner as shown previously. More reliance is placed on the solid portion of the lines but if this portion was extrapolated without regard to the other values obtained and used to obtain clinoenstatite activities, then it is found that clinoenstatite activities decrease with increasing mole fraction of clinoenstatite. In order to get a_{MS} increasing with increasing N_{MS} it is necessary for the iso-magnesia activity lines to curve sharply in the manner obtained.

Activities of Calcium Metasilicate obtained along the Clinoenstatite/Calcium Metasilicate join.

In the same manner as above it is possible to obtain activities of calcium metasilicate at 1550°C using the equation

$$CaO + SiO_2 = CS \quad \ldots\ldots\ldots\ldots \quad (21)$$

the free energy of formation of calcium metasilicate and lime and silica activities obtained from Figures 20 and 10 respectively.

Again the question arises as to which value should be used for the free energy of formation of calcium metasilicate. Kelley gives a value of -21,300 cal./mol. at 1550°C and when this is combined with the lime and silica activities, it gives, for mole fractions of calcium metasilicate of 0·5 and 0·75, activities of calcium metasilicate of 1·2 and 1·15 respectively. The free energy of formation of calcium metasilicate can be obtained from the modified results of Kay and Taylor [5] which are shown with the present results in Figures 10 and 20. At calcium metasilicate saturation on the $CaO-SiO_2$ binary, the activity of lime at 1550°C is given as 0·013 in Figure 20 and the activity of silica at 1550°C is given as 0·25 in Figure 10 and thus from equation (21), the free energy of formation of calcium metasilicate is obtained at 1550°C as - 20,700 cal./mol. As Kelley's value gave activities greater than 1, it was decided to use this value.

At $N_{CS} = 0·5$ ($CaO = 25·9$, $MgO = 16·7$, $SiO_2 = 55·4$), $a_{SiO_2} = 0·50$ from Figure 10 and $a_{CaO} = 0·007$ from Figure 20, hence $a_{CS} = 1·03$

At $N_{CS} = 0·75$ ($CaO = 37·4$, $MgO = 9·0$, $SiO_2 = 53·6$), $a_{SiO_2} = 0·40$ from Figure 10 and $a_{CaO} = 0·008$ from Figure 20, hence $a_{CS} = 0·96$.

Thus $N_{CS} = 0·5 \quad , \quad 0·75$

$a_{CS} = 1·03 \quad , \quad 0·96$

It is not possible to obtain a_{CS} at $N_{CS} = 0·25$ because the lime activities do not extend that far. It is noted that the calcium metasilicate activities decrease with increasing mole fraction and that the calcium metasilicate activity at mole fraction $N_{CS} = 0·5$ is greater than 1 but it is considered that within experimental error it is possible to adjust these values to give calcium metasilicate activities which remain constant at unit activity or decrease only slightly as the mole fraction of calcium metasilicate is decreased from 1 to 0·5.

Structure of the Liquid Melt in the $CaO-MgO-SiO_2$ System

In pure solid silica each silicon ion shares one electron charge with each of four oxygen ions forming a tetrahedron and electro-neutrality is obtained when each oxygen ion is shared by two tetrahedra. The structure of pure liquid silica is probably very similar, although it will be somewhat distorted in regularity. It is generally considered that when a basic oxide is added to this liquid each added oxygen ion breaks a corner between two tetrahedra while the cation enters an adjacent hole in the network. As more of the basic oxide is added the network is progressively broken down until SiO_4^{4-} anions are reached (orthosilicate composition) At any stage in this process a number of complex silicate anions will exist in the melt, including some SiO_4^{4-} anions and possibly some O^{2-} ions, although certain anion complexes will predominate at certain compositions.

From Figure 23 it can be seen that lime has a greater effect, mole for mole, in reducing in the activity of silica than has magnesia. This can be explained by an understanding of the structure of the liquid melt and an examination of the respective cation sizes and bond strengths. In order to break down the silica network each added oxygen ion must break a corner between two tetrahedra while the cation enters a hole in the silicate network. This requires the cation to increase its co-ordination from 6-fold to 12-fold, i.e. increase the length of the cation-oxygen bond and thus increase the energy of the system. The basic oxides tend to resist this and tend to form a two-liquid region giving a positive deviation from Raoultian behaviour. In the case of lime and magnesia considerable immiscibility exists in the binary silicate melts but the effect is greater in the case of magnesia due to a smaller cation size and increased cation-oxygen bond strength. Thus, considering equal molar additions of lime and magnesia, lime breaks down the silica network more effectively. This would appear to be the reason that the silica activity is decreased a greater amount by lime than by an equal molar addition of magnesia.

The $CaO-MgO-SiO_2$ system was examined with regard to Richardson's theory of ideal silicate mixing. This was dealt with briefly in the Introduction. For Richardson's model to hold the activities of the metasilicates must equal their respective mole fractions. The values obtained in the present results are

N_{MS} = 0·25 , 0·5 , 0·75
a_{MS} = 0·41 , 0·54 , 0·62
a_{CS} = 0·96 , 1·03 , -

It is obvious from the above data that Richardson's model does not hold in the $CaO-MgO-SiO_2$ system. This is not surprising because the model depends on the complex anion silicate structure being similar in both liquid metasilicates before mixing and as has just been shown, lime breaks down the silica network more effectively than magnesia, considering equal molar additions. At the metasilicate composition, the silicate anion structure is likely to be different for calcium metasilicate than for magnesium metasilicate (or clinoenstatite). Richardson's model appears to hold only for basic oxides whose cations are similar in size, e.g. the MnO-CaO-SiO_2 system.

Figure 23 shows silica, lime and magnesia activities on a molar basis and it was hoped that these results might give some other ideas about the structure of the melt in this system. However as can be seen from Figures 17 and 18 iso-magnesia activity lines are distorted upwards to a certain extent on approaching the liquidus surface, i.e. in Figure 18 the iso-magnesia activity lines have tended to straighten out with the retreat of the liquidus surface. At a high enough temperature it would be expected that magnesia activities would follow the line of periclase saturation (Figure 5). This effect was shown earlier in the discussion to occur in the iso-silica activity lines as well. In view of the limited liquid region in this system and the effect that this has on the iso-activity lines of silica and magnesia it is considered that it would be unwise to speculate on the structure of the melt.

FIG. 23

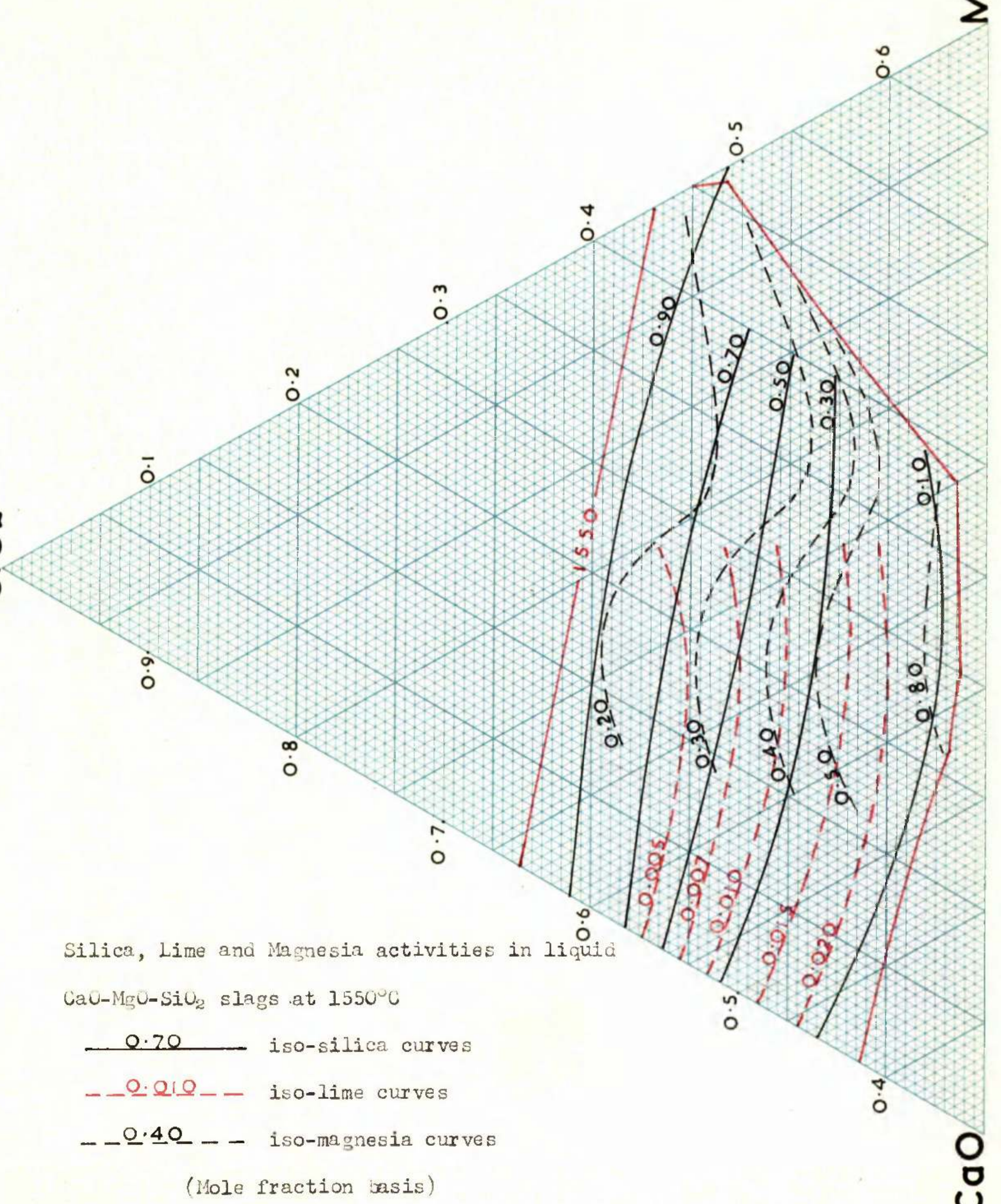

Silica, Lime and Magnesia activities in liquid

CaO-MgO-SiO_2 slags at 1550°C

0·70 iso-silica curves

0·010 iso-lime curves

0·40 iso-magnesia curves

(Mole fraction basis)

Summary of interoxide free energy data given by Kelley showing compatibility and incompatibility.

In this section of the discussion Kelley's data will be compared with the free energy data obtained from the results of the present investigation and it will be shown that some of Kelley's data show incompatibility whereas all the data obtained from the present results show compatibility.

Consider the following equation

$$C_2S \; + \; CMS \; = \; C_3MS_2 \qquad \ldots\ldots\ldots\ldots \qquad (22)$$

Kelley's data gives the sum of the free energies of formation of calcium orthosilicate and monticellite at 1550°C as - 60·9 Kcal./mol. and the free energy of formation of merwinite at this temperature as - 55·3 K cal./mol. This would mean that merwinite would be unstable with respect to calcium orthosilicate and monticellite. Therefore these data are incompatible with each other. The data obtained from the present work give the sum of the interoxides on the left hand side of equation (22) as - 55·6 K cal./mol. and the free energy of formation of merwinite as - 56·5 K cal/mol. showing compatability.

Now consider equation (23)

$$\text{i.e. } CS \; + \; CMS \; = \; C_2MS_2 \qquad \ldots\ldots\ldots\ldots \qquad (23)$$

Kelley's data gives the sum of the free energies of formation of calcium metasilicate and monticellite as - 48·1 K.cal./mol. and the free energy of formation of akermanite as - 43·0 K.cal./mol. again showing incompatibility. The data given by the present work are - 42·1 K cal./mol. and - 42·9 K cal./mol. respectively showing compatibility. Monticellite is common to both equations (22) and (23) and is therefore suspected to be unreliable.

In the following equations Kelley's free energy data is given below the interoxide compounds with the data obtained from the present work in brackets alongside. The data for the compounds on the left hand side of each equation have been summed. It can be seen that some of Kelley's data show incompatibility whereas all the data obtained in the present work show compatibility.

C_2S + MS = C_2MS_2 .... (24)
-41·4 (-38·6) -43·0(-42·9)

C_2S + M_2S = $2CMS$ .... (25)
-49·1 (-43·1) -53·4(-43·0)

3_2S + M_2S = $2C_3MS_2$ ...... (26)
-117·3(-111·3) -110·6(-113·0)

TABLE 9 Comparison of the Free Energy Data.

Compound	Kelley's Value cal./mol.	Present work cal./mol
M_2S	-15,100	-9,000
MS	- 7,300	-4,700
C_3MS_2	-55,250	-56,500
CMS	-26,800	-21,500
CMS_2	-32,900	-28,000
C_2MS_2	-43,000	-42,900

$$CS + MS = CMS_2 \quad .... \quad (27)$$

$$-28{\cdot}6(-25{\cdot}1) \qquad -32{\cdot}9(-28{\cdot}0)$$

Table 9 gives a comparison of all the free energy of formation data obtained from the present work with the data given by Kelley.

THE $MgO-Al_2O_3-SiO_2$ SYSTEM

Comparison with Rein and Chipman [26]

Rein and Chipman have investigated the $MgO-Al_2O_3-SiO_2$ system by equilibrating liquid slags with liquid Fe-Si-C alloys in silicon carbide crucibles at 1600°C in CO gas according to the equation

$$SiO_2(\text{slag}) + 2SiC(\text{crucible}) = 3\underline{Si}(\text{in Fe}) + 2CO(g)...(28)$$

With carbon monoxide gas at 1 atmosphere the equilibrium constant for this reaction reduces to $K_{28} = a^3\,Si/a_{SiO_2}$. This equilibrium constant K_{28} can be obtained from the free energy data for silica, silicon carbide and carbon monoxide. As before, the data obtained by Rein and Chipman were presented in the form of lines of constant silicon content in the metal which are also lines of constant silica activity in the slag. In this case a difficulty was met when an attempt was made to convert the values of constant silicon content given by Rein and Chipman to values of silica activities.

Data exist giving the graphite content of graphite saturated Fe-Si-C melt for a range of silicon content up to 22·4% Si where the metal phase is saturated both with graphite and silicon carbide [35]. At greater silicon contents no data exist and the results obtained by Rein and Chipman in the $MgO-Al_2O_3-SiO_2$ system are all greater than 22·4% Si.

It was first thought that as the graphite content was very small it would not affect the activity of silicon and thus the activity of silica by very much and the system was considered as a binary Fe-Si melt and silica activities obtained. Then, in order to see the effect of graphite on these activities, the data for graphite saturation was extrapolated and used to obtain silica activities in the Fe-Si-C melt. The true activities would lie somewhere between the values just obtained. It was obvious from the results obtained that graphite content influenced silica activity to a greater extent than was first thought, e.g. at 24·5%Si the true activity of silica lies between 0·39 - 0·55. It was then realised that this was due to the fact that the equilibrium constant for equation (28) is $K_{28} = a^{2}Si/a_{SiO_2}$. Therefore a small error in the activity of silicon gives a much larger error in the activity of silica.

As can be seen from Figure 16 the shape of the curves do not agree with those obtained in the present investigation.

No values have been given for these iso-activity lines for the above reason but if the most basic line is taken as lying somewhere between 0·39 - 0·55 silica activity, then it can be seen that the results obtained by Rein and Chipman show a more rapid decrease in silica activity as additions of magnesia and alumina are made than the results obtained in the present investigation.

No other thermodynamic data are available to compare with the present results, neither activity data nor free energy of interoxide data. It was decided to use the present results in two ways, first of all they can be used to obtain magnesia and alumina activities by the Gibbs-Schumann integration, and secondly they can be used to obtain estimates of the free energies of formation of some of the interoxide compounds.

<u>Magnesia Activities at 1550°C</u>

A starting point for the Gibbs-Schumann integration was chosen on the binary eutectic trough between forsterite and spinel (Figure 11) at 1550°C (i.e. $MgO = 33 \cdot 6$, $Al_2O_3 = 22 \cdot 6$, $SiO_2 = 43 \cdot 8$). The silica activity at this point was obtained from the iso-silica activity lines in Figure 16 by plotting silica activity against weight percent silica at a constant magnesia content of 22·6 wt. % and extrapolating. This gave a silica activity of 0·39. Now at this point the slag is saturated with respect to forsterite and therefore the following equation can be used to obtain the magnesia activity of the slag.

$$\text{i.e.} \quad M_2S \; = \; 2MgO + SiO_2 \; \ldots\ldots\ldots \quad (11)$$

The equilibrium constant for reaction (11) is $K_{11} = a^2_{MgO} . a_{SiO_2}$ and using the free energy of formation of forsterite which was obtained earlier then

$$2 \log a_{MgO} \; = \; - \frac{9000}{4{\cdot}575 \times 1823} - \log a_{SiO_2}$$

$$\text{thus} \quad a_{MgO} \; = \; 0{\cdot}46$$

It is now possible to carry out the Gibbs-Schumann integration and the results are shown in Figure 21. The working data are given in Table K in the appendix.

Extension of Magnesia Activities at 1550°C

Magnesia activities were now obtained along the forsterite saturation boundary at 1550°C. Again it is possible to use the equation

$$M_2S \; = \; 2MgO + SiO_2 \; \ldots\ldots\ldots\ldots\ldots \quad (11)$$

Three points were chosen along this line and silica activities were obtained at these points from Figure 16 and as before the magnesia activities were calculated.

FIG. 21

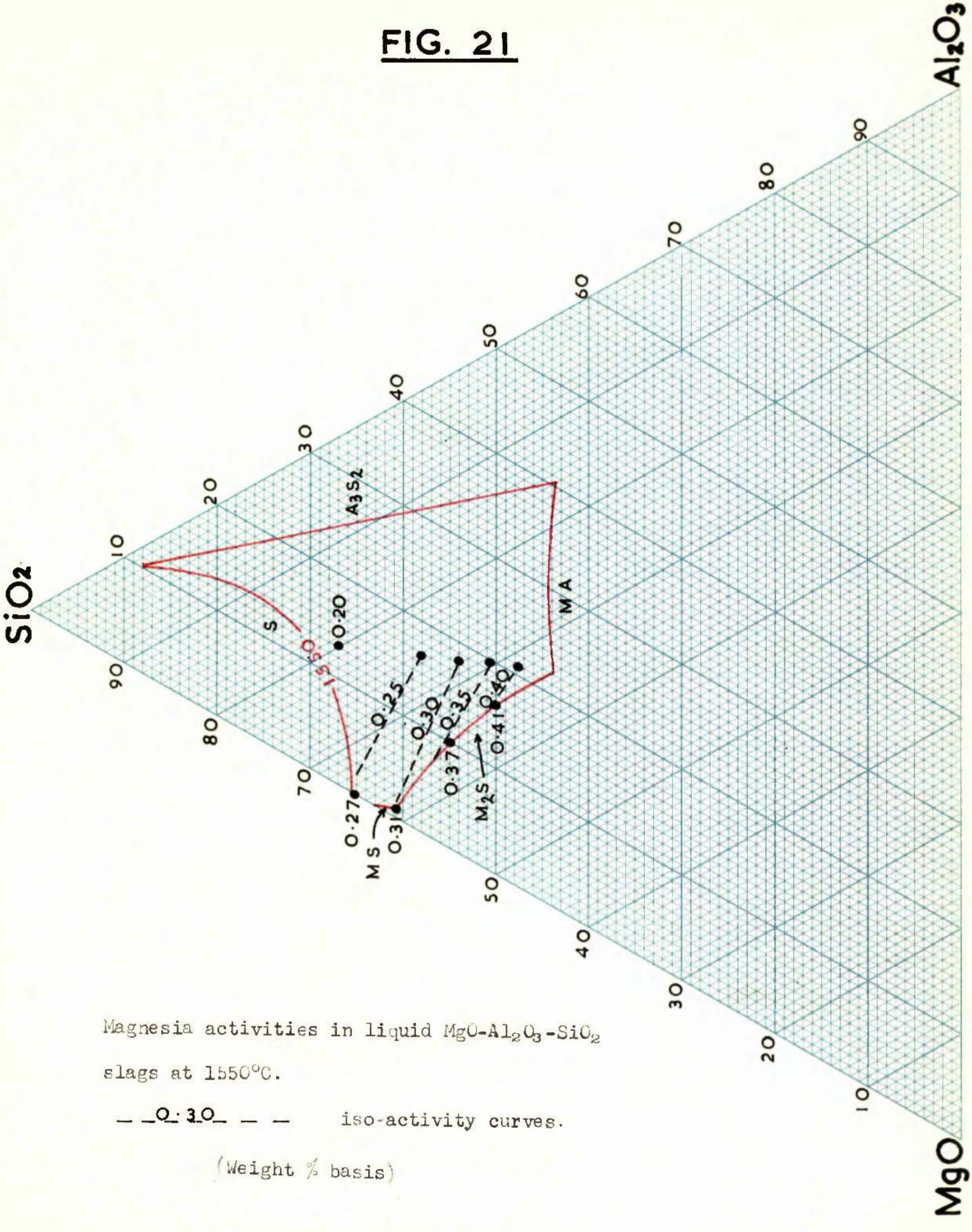

Magnesia activities in liquid MgO-Al_2O_3-SiO_2 slags at 1550°C.

— —0·30— — — iso-activity curves.

(Weight % basis)

At point ($MgO = 34\cdot0$, $Al_2O_3 = 16\cdot0$, $SiO_2 = 50\cdot0$), the silica activity = 0·5. From equation (11)

$$2 \log a_{MgO} = - \frac{9000}{4\cdot575 \times 1823} - \log a_{SiO_2}$$

$$\text{thus } a_{MgO} = 0\cdot41$$

At point ($MgO = 35\cdot0$, $Al_2O_3 = 10\cdot0$, $SiO_2 = 55\cdot0$), the silica activity = 0·62 giving $a_{MgO} = 0\cdot37$.

At point ($MgO = 38\cdot3$, $Al_2O_3 = 1\cdot0$, $SiO_2 = 60\cdot7$), the silica activity = 0·88 giving $a_{MgO} = 0\cdot31$.

It is also possible to obtain the magnesia activity at 1543°C on the binary eutectic trough between clinoenstatite and tridymite. At this point ($MgO = 34\cdot9$, $SiO_2 = 65\cdot1$) the silica activity = 1·0, and the following equation can be used to obtain the magnesia activity

$$\text{i.e. } MS = MgO + SiO_2 \quad \ldots\ldots\ldots \quad (20)$$

Using the free energy of formation of clinoenstatite obtained earlier

$$\log a_{MgO} = - \frac{4,700}{4\cdot575 \times 1816}$$

$$\text{thus } a_{MgO} = 0\cdot27$$

The magnesia activities just obtained are plotted with those obtained by the Gibbs-Schumann integration in Figure 21.

Alumina Activities at 1550°C

Again the starting point for the Gibbs-Schumann integration was chosen on the binary eutectic trough between forsterite and spinel at 1550°C (i.e. MgO = 33·6, Al_2O_3 = 22·6, SiO_2 = 43·8). The silica activity at this point was obtained as 0·39. As the slag is saturated with respect to both forsterite and spinel, the following equation holds

$$\text{i.e.} \quad 2MA + SiO_2 = M_2S + 2Al_2O_3 \quad \ldots\ldots \qquad (29)$$

Now the free energy change for reaction (29) is obtained from the free energies of formation of forsterite and spinel

$$\text{i.e.} \quad \Delta G^\circ_{29} = \Delta G^\circ_{M_2S} - 2\Delta G^\circ_{MA}$$

The free energy of formation of forsterite was determined earlier in this discussion and the free energy of formation of spinel was obtained from Kalyanram and Bell [36] recalculated in the light of new data [37]

$$\text{i.e.} \quad \Delta G^\circ_{29} = -9000 - 2(-3{,}830)$$

$$= -1{,}340 \text{ cal./mol.}$$

The equilibrium constant for reaction (29) is $K_{29} = a^2{}_{Al_2O_3}/a_{SiO_2}$

$$\text{therefore} \quad 2 \log a_{Al_2O_3} = \frac{1{,}340}{4{\cdot}575 \times 1823} + \log a_{SiO_2}$$

$$\text{thus} \quad a_{Al_2O_3} = 0{\cdot}75$$

The Gibbs-Schumann integration was now carried out and the results are shown in Figure 22. The working data are given in Table L in the appendix.

Extension of Alumina Activities at 1550°C

Alumina activities can be obtained along the line of mullite saturation at 1550°C. The following equation was used

$$\text{i.e.} \quad A_3S_2 \;=\; 3Al_2O_3 + 2SiO_2 \quad \ldots\ldots\ldots \quad (30)$$

The free energy of formation of mullite at 1550°C was obtained from Kay and Taylor [5] as - 5,300 cal./mol. and silica activities were obtained along the line of mullite saturation at 1550°C from Figure 16. Alumina activities were then obtained from the equation

$$3 \log a_{Al_2O_3} \;=\; - \frac{5{,}300}{4{\cdot}575 \times 1823} - 2 \log a_{SiO_2}$$

At point ($MgO = 14{\cdot}5$, $Al_2O_3 = 37{\cdot}3$, $SiO_2 = 48{\cdot}2$) where the silica activity = 0·7, $a_{Al_2O_3} = 0{\cdot}77$.

At point ($MgO = 12{\cdot}7$, $Al_2O_3 = 33{\cdot}3$, $SiO_2 = 54{\cdot}0$) where the silica activity = 0·8, $a_{Al_2O_3} = 0{\cdot}72$.

At point ($MgO = 10{\cdot}6$, $Al_2O_3 = 29{\cdot}4$, $SiO_2 = 60{\cdot}0$) where the silica activity = 0·9, $a_{Al_2O_3} = 0{\cdot}66$.

Finally, at point ($MgO = 1{\cdot}5$, $Al_2O_3 = 11{\cdot}5$, $SiO_2 = 88{\cdot}0$) where the silica activity = 1·0(silica saturation) $a_{Al_2O_3} = 0{\cdot}61$

These values of alumina activities are shown with the activities obtained by the Gibbs-Schumann integration in Figure 22.

FIG. 22

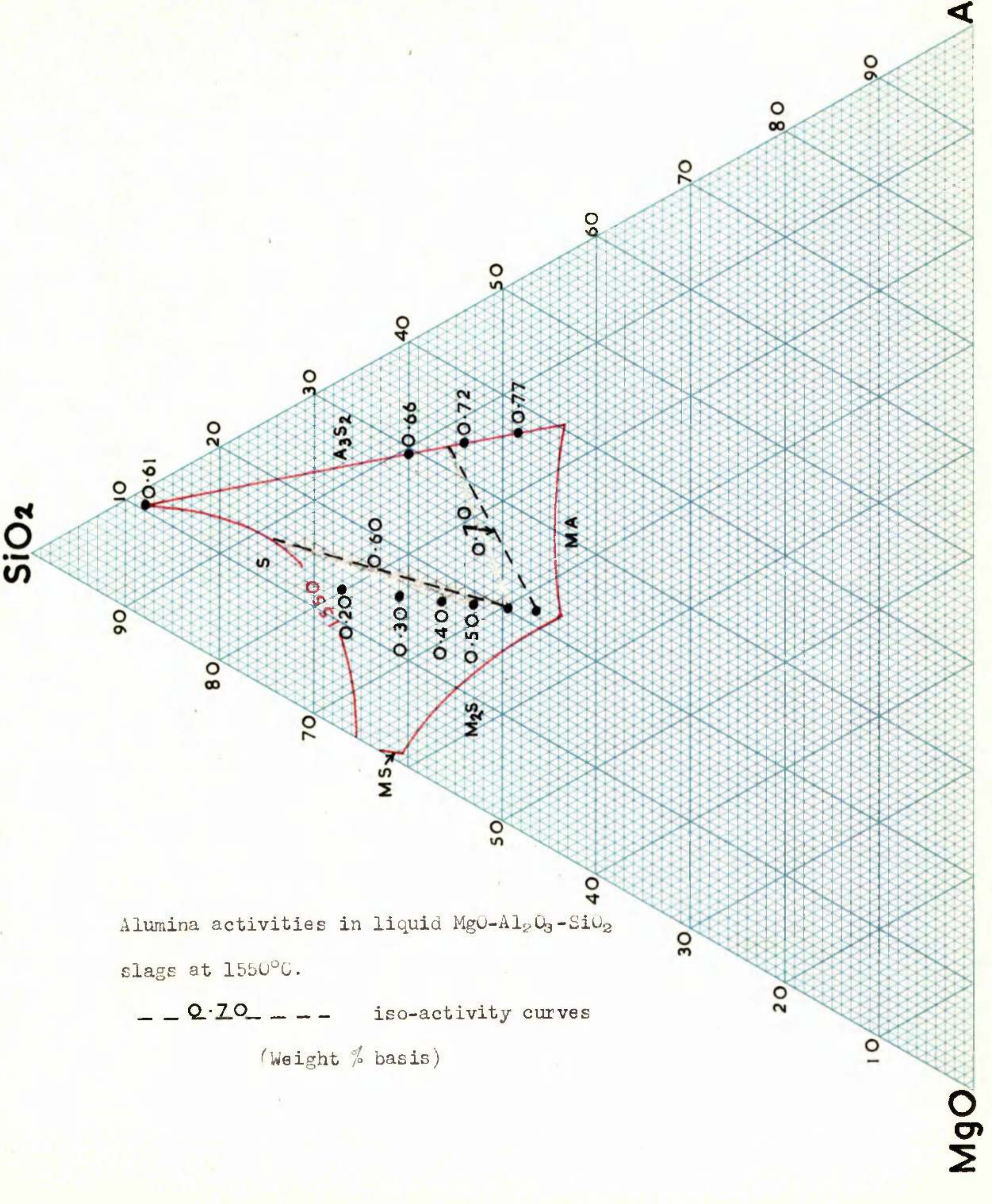

Alumina activities in liquid $MgO-Al_2O_3-SiO_2$ slags at 1550°C.

_ _ 0·70_ _ _ _ iso-activity curves

(Weight % basis)

The Free Energy of Formation of Sapphirine ($M_4A_5S_2$)

At 1482°C ($MgO = 16{\cdot}8$, $Al_2O_3 = 36{\cdot}8$, $SiO_2 = 46{\cdot}4$) the liquid slag is saturated with respect to mullite, spinel and sapphirine and a peritectic reaction takes place. This can be represented by the equation

$$12MA + A_3S_2 + 4SiO_2 = 3M_4A_5S_2 \; \ldots\ldots \qquad (31)$$

The activity of silica at this point was obtained from the iso-activity lines at 1500° C (Figure 15) and the temperature coefficient which was determined from Figure 16. This gave an activity of silica = 0·7. The free energy change for reaction (31) was now determined.

$$\text{i.e.} \quad \Delta G_{31} = -4{\cdot}575 \times 1755 \times 4(-\log 0{\cdot}7)$$

$$\underline{\Delta G_{31} = -5{,}000 \text{ cal./mol.}}$$

Also

$$\Delta G_{31} = 3\,\Delta G^{\circ}_{M_4A_5S_2} - 12\Delta G^{\circ}_{MA} - \Delta G^{\circ}_{A_3S_2}$$

$$\therefore \quad 3\,\Delta G^{\circ}_{M_4A_5S_2} = -5{,}000 + 12(-3{,}800) + (-4{,}000)$$

$$= -54{,}600$$

$$\underline{\therefore \Delta G^{\circ}_{M_4A_5S_2} = -18{,}200 \text{ cal./mol.}}$$

The Free Energy of Formation of Cordierite ($M_2A_2S_5$)

At 1460°C, ($MgO = 16{\cdot}4$, $Al_2O_3 = 34{\cdot}5$, $SiO_2 = 49{\cdot}1$) the liquid slag is saturated with respect to mullite, sapphirine and cordierite and a peritectic reaction takes place. This can be represented by the equation

$$3M_4A_5S_2 + 26SiO_2 = 6M_2A_2S_5 + A_3S_2 \quad ....(32)$$

The activity of silica at this point is obtained as before giving $a_{SiO_2} = 0{\cdot}80$. The free energy change for the above reaction (32) was now determined.

$$\text{i.e.} \quad \Delta G_{32} = -4{\cdot}575 \times 1733 \times 26(-\log 0{\cdot}8)$$

$$\underline{\Delta G_{32} = -20{,}400 \text{ cal./mol.}}$$

Also $\quad \Delta G_{32} = 6\Delta G^{\circ}_{M_2A_2S_5} + \Delta G^{\circ}_{A_3S_2} - 3\Delta G^{\circ}_{M_4A_5S_2}$

$$\therefore 6\Delta G^{\circ}_{M_2A_2S_5} = -20{,}400 + 3{,}700 - 54{,}600$$

$$= -71{,}300$$

$$\underline{\Delta G^{\circ}_{M_2A_2S_5} = -12{,}000 \text{ cal./mol.}}$$

REFERENCES.

REFERENCES

1. L.C. Chang and G. Derge — Trans. Amer. Inst. Min.(metall.) Engrs. 1947, Vol. 172, p. 90.

2. P.T. Carter and T.G. MacFarlane J. Iron St. Inst., 1957, Vol. 185, p.54

3. L. Yang, C.L. McCabe and R. Miller, Physical Chemistry of Steelmaking, New York, John Wiley, 1958, p.63.

4. R.A. Sharma and F.D. Richardson, J. Iron St. Inst., 1961, Vol.198, p.386; ibid, 1962, Vol.200, p.373.

5. D.A.R. Kay and J. Taylor — Trans. Faraday Soc., 1960, Vol.56, p. 1372.

6. K. Sanbongi and Y. Omori — Physical Chemistry of Metallic Solutions and Intermetallic Compounds, London, N.P.L. Vol. 2, 1959, Paper 60.

7. J. Chipman — Physical Chemistry of Process Metallurgy, Interscience, 1961, p. 27.

8. R. Schumann and P.J. Ensio — Trans. Amer. Inst. min.(metall.) Engrs., 1951, Vol. 191, p.401.

9. C. Bodsworth — J. Iron St. Inst., 1959, Vol.193, p.13.

10. K.P. Abraham, M.W. Davies and F.D. Richardson - J. Iron St. Inst., 1960, Vol. 196, p.82.

11. F.D. Richardson — The Physical Chemistry of Steelmaking, Technology Press, M.I.T., 1958, p. 59.

12. K.L. Fetters and J. Chipman — Am. Inst Mining Met. Engrs. Tech. Publ. 13 (1941)

13. C.R. Taylor and J. Chipman — Ibid, 1499 (1942)

14. H.L. Bishop, N.J. Grant and J. Chipman Trans. Amer. Inst. min.(metall.) Engrs., 1950, Vol. 212, p. 185.

15. F.D. Richardson and T.C.M. Pillay Trans. Inst. Mining Met.(London) 66, 309 (1956-57).

16. F.D. Richardson, — Trans. Faraday Soc., 52, 1312 (1956).

17. E.J. Michal and R. Schuhmann — J. Metals, 1956, Vol. 4, p. 723.

18. E.T. Turkdogan and J. Pearson J. Iron and St. Inst., 1953, Vol. 175, p.393.

19. K.P. Abraham and F.D. Richardson Physical Chemistry of Process Metallurgy A.I.M.M.E., Interscience, 1961, p.263.

20. H.B. Bell J. Iron St. Inst., 1961, Vol. 197, p.245.

21. H. Flood, T. Forland and K. Grjotheim Physical Chemistry of Melts, London, Inst. Min. Met., 1953, p. 46.

22. H. Flood and K. Grjotheim J. Iron St. Inst., 1952, Vol. 171, p.64.

23. J. Lumsden Physical Chemistry of Process Metallurgy, A.I.M.M.E., Interscience, 1961, p. 165.

25. E.F. Osborn and A. Muan Phase Equilibrium Diagrams of Oxide Systems, Amer. Cer. Soc., 1960.

26. R.H. Rein and J. Chipman Trans. A.I.M.E. (in the press).

27. R. Baschwitz and J. Chipman Trans. A.I.M. E. (in the press)

28. J. Hager Trans. A.I.M. E., 1963, Vol.227, p. 1000.

29. G.M. Smith and J. Taylor J.I.S.I. (in the press)

30. K.K. Kelley Heats and Free Energies of Formation of Anhydrous Silicates, U.S. Bureau of Mines, 1962, No. 5901.

31. K.K. Kelley High Temperature Heat-Content, Heat-Capacity, and Entropy Data for the Elemen and Inorganic Compounds, U.S. Bureau of Mines, 1960, No. 584.

32. K.K. Kelley and E.G. King Entropies of the Elements and Inorganic Compounds, U.S. Bureau of Mines, 1961, No. 592.

33. E.G. King Jour. Am. Chem. Soc., 1951, Vol. 73, p.65

34. K. Sawamura Tetsu-To-Hagane (overseas), 1962, Vol.2, No. 3, p.3.

35. J. Chipman, J.C. Fulton, N. Gokcen and G.R. Caskey, Acta. Met. 1954, Vol. 2, p. 439.

36. M.R. Kalyanram and H.B. Bell Trans. Brit. Ceram. Soc., 1961, Vol. 60, p. 135.

37. T.B. Gibbons Private communication.

38. J.F. Elliot and M. Gleiser Thermochemistry for Steelmaking, 1960, Vol. 1.

39. W.D. Good J. Chem. Phys., 1962, Vol. 66, p. 380.

40. S.S. Wise, J.L. Margrave, H.M. Feder and W.N. Hubbard, J. Chem. Phys., 1962, Vol. 66, p. 381.

APPENDIX

THERMODYNAMIC DATA

and

WORKING DATA

THERMODYNAMIC DATA

The reaction $Si\ (l)\ +\ O_2(g)\ =\ SiO_2\ (\beta\ crist.)$

The free energy of formation of cristobalite is given in tabular form by Elliot and Gleiser [38]. These data have been modified in the light of new determinations of the heat of formation of silica [39, 40] and the modified data may be represented in the temperature range 1686 - 1900°K by the linear equation

$$\Delta G^{\circ}_{T} = -226{,}900 + 47{\cdot}6\ T\ \text{cals./mol} \ldots\ldots (A)$$

The reaction $Si\ (l)\ +\ \frac{1}{2}O_2(g)\ =\ SiO(g)$

The free energy of formation of silicon monoxide is given in tabular form by Elliot and Gleiser. These data have also been modified to take into account the new determinations of the heat of formation of silica and the modified data may be represented in the temperature range 1686 - 1900°K by the linear equation

$$\Delta G^{\circ}_{T} = -40{,}200 - 11{\cdot}22\ T\ \text{cals./mol} \ldots\ldots\ldots (B)$$

The reaction $C(gr)\ +\ \frac{1}{2}O_2(g)\ =\ CO(g)$

The free energy of formation of carbon monoxide is also given in tabular form by Elliot and Gleiser and may be represented in the temperature range 1600 - 1900°K by the linear equation

$$\Delta G^\circ_T = -28{,}000 - 20{\cdot}24\ T \text{ cals./mol} \quad ....(C)$$

<u>The reaction SiO_2 (β crist.) + C(gr) = CO(g) + SiO(g)</u>

The free energy change for the above reaction is obtained from equations A, B and C and may be represented in the temperature range 1686 - 1900°K by the linear equation

$$\Delta G^\circ_T = +\ 156{,}700 - 79{\cdot}06\ T \text{ cals./mol} \quad ......(D)$$

TABLE A Magnesia activities at 1500°C in the CaO-MgO-SiO_2 system.

(starting point is CaO = 32·5, MgO = 26·2, SiO_2 = 41·3)

a_{SiO_2}	$-\ln a_{SiO_2}$	Wt % SiO_2/Wt % MgO	N_{SiO_2}/N_{MgO}	$-\ln a_{MgO}$	a_M
0·065	2·7334	54/46	0·785	0·00	1·
0·2	1·6095	52/48	0·725	0·8430	0·
0·3	1·2040	52·5/47·5	0·735	1·1408	0·
0·4	0·9163	52·5/47·5	0·735	1·3452	0·
0·5	0·6932	52·5/47·5	0·735	1·5142	0·
0·6	0·5108	54/46	0·785	1·6506	0·
0·7	0·3567	55·5/44·5	0·835	1·7712	0·
0·8	0·2232	56/42	0·925	1·8922	0·
0·9	0·1054	62/38	1·090	2·0016	0·

TABLE B Magnesia activities at 1500°C in the CaO-MgO-SiO_2 system.

(starting point is CaO = 37·5, MgO = 22·3, SiO_2 = 40·2)

a_{SiO_2}	$-\ln a_{SiO_2}$	Wt % SiO_2/Wt % MgO	N_{SiO_2}/N_{MgO}	$-\ln a_{MgO}$	a_{MgO}
0·1	2·3026	48/52	0·615	0·00	1·0
0·2	1·6095	49/51	0·64	0·4154	0·65
0·3	1·2040	49·5/50·5	0·655	0·6756	0·50
0·4	0·9163	50/50	0·665	0·8596	0·42
0·5	0·6932	51/49	0·695	1·0148	0·36
0·6	0·5108	54/46	0·785	1·1498	0·31
0·7	0·3567	56·5/43·5	0·865	1·2920	0·27
0·8	0·2232	58·5/41·5	0·94	1·4186	0·24
0·9	0·1054	62/38	1·09	1·5116	0·22

TABLE C Magnesia activities at 1500°C in the $CaO-MgO-SiO_2$ system.

(starting point is CaO = 47·0, MgO = 11·3, SiO_2 = 41·7)

a_{SiO_2}	$-\ln a_{SiO_2}$	Wt % SiO_2/Wt % MgO	N_{SiO}/N_{MgO}	$-\ln a_{MgO}$	a_{MgO}
0·135	2·0025	34/66	0·345	0·7134	0·49
0·2	1·6095	37/63	0·395	0·8550	0·43
0·3	1·2040	40/60	0·445	1·0236	0·36
0·4	0·9163	44·5/55·5	0·540	1·1610	0·31
0·5	0·6932	49·5/50·5	0·655	1·2980	0·27
0·6	0·5108	54/46	0·790	1·4454	0·24
0·7	0·3567	57·5/42·5	0·900	1·5696	0·21
0·8	0·2232	60/40	1·005	1·7040	0·18
0·9	0·1054	63·5/36·5	1·17	1·8246	0·16

TABLE D Magnesia activities at 1550°C in the $CaO-MgO-SiO_2$ system (starting point is $CaO = 29·0$, $MgO = 29·8$, $SiO_2 = 41·2$).

a_{SiO_2}	$-\ln a_{SiO_2}$	Wt % SiO_2/Wt % MgO	N_{SiO_2}/N_{MgO}	$-\ln a_{MgO}$	a_{MgO}
0·065	2·7334	49/51	0·64	0·00	1·00
0·1	2·3026	50/50	0·67	0·2804	0·76
0·2	1·6095	51·4/48·6	0·705	0·755	0·47
0·3	1·2040	51·4/48·6	0·705	1·054	0·35
0·4	0·9163	51·8/48·2	0·715	1·2036	0·30
0·5	0·6932	54/46	0·78	1·3742	0·25
0·6	0·5108	55/45	0·815	1·5156	0·22
0·7	0·3567	57/43	0·885	1·6426	0·19
0·8	0·2232	60/40	1·00	1·7732	0·17
0·9	0·1054	63/37	1·135	1·8894	0·15

TABLE 8 Magnesia activities at 1550°C in the $CaO-MgO-SiO_2$ system

(starting point is $CaO = 40·8$, $MgO = 20·0$, $SiO_2 = 39·2$)

a_{SiO_2}	$-\ln a_{SiO_2}$	Wt % SiO_2/Wt % MgO	N_{SiO_2}/N_{MgO}	$-\ln a_{MgO}$	a_{MgO}
0·08	2·5258	40·5/59·5	0·455	0·00	1·0
0·1	2·3026	41·5/58·5	0·475	0·1052	0·9
0·2	1·6095	46/54	0·570	0·4648	0·63
0·3	1·2040	48/52	0·615	0·7172	0·49
0·4	0·9163	50·5/49·5	0·680	0·8876	0·41
0·5	0·6932	52·5/47·5	0·735	1·0496	0·35
0·6	0·5108	56/44	0·85	1·1912	0·3
0·7	0·3567	59/41	0·96	1·3254	0·27
0·8	0·2232	61/39	1·04	1·4662	0·23
0·9	0·1054	64/36	1·19	1·5888	0·2

TABLE F Lime activities at 1500°C in the $CaO-MgO-SiO_2$ system

(starting point is CaO = 47·9, MgO = 10·0, SiO_2 = 42·1)

a_{SiO_2}	$-\ln a_{SiO_2}$	Wt % SiO_2/Wt % CaO	N_{SiO_2}/N_{CaO}	$-\ln a_{CaO}$	a_{CaO}
0·135	2·0025	43·5/56·5	0·72	3·8167	0·022
0·2	1·6095	45·5/54·5	0·78	4·1103	0·016
0·3	1·2040	50/50	0·93	4·4591	0·012
0·4	0·9163	52·5/47·5	1·03	4·7297	0·0088
0·5	0·6932	54·5/45·5	1·12	4·9751	0·0069
0·6	0·5108	56/44	1·19	5·1833	0·0056
0·7	0·3567	57·5/42·5	1·26	5·3681	0·0047
0·8	0·2232	59·5/40·5	1·37	5·5519	0·0039
0·9	0·1054	61·5/38·5	1·49	5·7075	0·0033

TABLE G Lime activities at 1500°C in the CaO-MgO-SiO_2 system.

(starting point is CaO = 39·3, MgO = 20·0, SiO_2 = 40·7)

a_{SiO_2}	$-\ln a_{SiO_2}$	Wt % SiO_2/Wt % CaO	N_{SiO_2}/N_{CaO}	$-\ln a_{CaO}$	a_{CaO}
0·115	2·1628	39/61	0·595	3·7297	0·024
0·2	1·6095	42/52	0·675	4·0857	0·017
0·3	1·2040	47·5/52·5	0·845	4·4027	0·012
0·4	0·9163	51·0/49·0	0·970	4·6567	0·0095
0·5	0·6932	54·0/46	1·095	4·8911	0·0075
0·6	0·5108	56·0/44	1·190	5·0927	0·0061
0·7	0·3567	58·0/42	1·290	5·2867	0·0051
0·8	0·2232	60/40	1·40	5·4645	0·0042
0·9	0·1054	62/38	1·52	5·6253	0·0036

TABLE H Lime activities at 1500°C in the CaO-MgO-SiO_2 system

(starting point is CaO = 32·5, MgO = 26·2, SiO_2 = 41·3)

a_{SiO_2}	$-\ln a_{SiO_2}$	Wt % SiO_2/Wt % CaO	N_{SiO_2}/N_{CaO}	$-\ln a_{CaO}$	a_{CaO}
0·065	2·7334	24/76	0·294	3·2969	0·037
0·2	1·6095	38/62	0·570	3·7841	0·023
0·3	1·2040	44·5/55·5	0·750	4·0517	0·017
0·4	0·9163	49/51	0·895	4·2791	0·014
0·5	0·6932	53/47	1·050	4·5011	0·011
0·6	0·5108	56·5/43·5	1·210	4·7005	0·0091
0·7	0·3567	58·5/41·5	1·315	4·8879	0·0075
0·8	0·2232	60·5/39·5	1·430	5·0817	0·0062
0·9	0·1054	63/37	1·59	5·2369	0·0053

TABLE I Lime activities at 1550°C in the $CaO-MgO-SiO_2$ system

(starting point is CaO = 46·6, MgO = 10·0, SiO_2 = 41·4).

a_{SiO_2}	$-\ln a_{SiO_2}$	Wt % SiO_2/Wt % CaO	N_{SiO_2}/N_{CaO}	$-\ln a_{CaO}$	a_{CaO}
0·08	2·5258	43/57	0·710	3·4420	0·032
0·1	2·3026	44·5/55·5	0·725	3·6090	0·027
0·2	1·6095	48·5/51·5	0·88	4·1660	0·016
0·3	1·2040	52·5/47·5	1·02	4·5550	0·011
0·4	0·9163	54·5/45·5	1·10	4·8528	0·0078
0·5	0·6932	56·5/43·5	1·21	5·1126	0·0060
0·6	0·5108	58·0/42	1·30	5·3358	0·0048
0·7	0·3567	59·5/40·5	1·37	5·5348	0·0039
0·8	0·2232	61·5/38·5	1·47	5·7348	0·0032
0·9	0·1054	63·5/36·5	1·61	5·9048	0·0027

TABLE J Lime activities at 1550°C in the $CaO-MgO-SiO_2$ system

(starting point is CaO = 41·5, MgO = 19·0, SiO_2 = 39·5)

a_{SiO_2}	$-\ln a_{SiO_2}$	Wt % SiO_2/Wt % CaO	N_{SiO_2}/N_{CaO}	$-\ln a_{CaO}$	a_{CaO}
0·08	2·5258	40·5/59·5	0·635	3·4420	0·032
0·1	2·3026	42/58	0·675	3·5910	0·027
0·2	1·6095	46/54	0·795	4·1042	0·017
0·3	1·2040	51/49	0·97	4·4740	0·011
0·4	0·9163	54·5/45·5	1·12	4·7628	0·0085
0·5	0·6932	56·5/43·5	1·21	5·0250	0·0066
0·6	0·5108	58/42	1·29	5·2478	0·0051
0·7	0·3567	59·5/40·5	1·37	5·4476	0·0043
0·8	0·2232	61·5/38·5	1·49	5·6488	0·0035
0·9	0·1054	64/36	1·66	5·8218	0·0030

TABLE K Magnesia activities at 1550°C in the $MgO-Al_2O_3-SiO_2$ system
(starting point is $MgO = 33\cdot6$, $Al_2O_3 = 22\cdot6$, $SiO_2 = 43\cdot8$)

a_{SiO_2}	$-\ln a_{SiO_2}$	Wt % SiO_2/Wt % MgO	N_{SiO_2}/N_{MgO}	$-\ln a_{MgO}$	$-\ln a_{MgO}$
0·39	0·9416	50·5/49·5	0·685	0·7765	0·46
0·5	0·6932	55/45	0·820	0·9652	0·38
0·6	0·5108	57·5/42·5	0·910	1·1213	0·33
0·7	0·3567	60/40	1·01	1·3093	0·27
0·8	0·2232	60·5/39·5	1·03	1·4545	0·23
0·9	0·1054	62/38	1·095	1·5727	0·21

TABLE 1 Alumina activities at 1550°C in the MgO-Al_2O_3-SiO_2 system

(starting point is $MgO = 33\cdot6$, $Al_2O_3 = 22\cdot6$, $SiO_2 = 43\cdot8$).

a_{SiO_2}	$-\ln a_{SiO_2}$	Wt % SiO_2/Wt % Al_2O_3	$N_{SiO_2}/N_{Al_2O_3}$	$-\ln a_{Al_2O_3}$	$a_{Al_2O_3}$
0·39	0·9416	29/71	0·695	0·2877	0·75
0·5	0·6932	35·5/64·5	0·935	0·4887	0·61
0·6	0·5108	41·0/59·0	1·180	0·6601	0·52
0·7	0·3567	48·5/51·5	1·60	0·8627	0·42
0·8	0·2232	59/41	2·445	1·1387	0·32
0·9	0·1054	69/31	3·80	1·4687	0·23

ACKNOWLEDGMENTS

This research was carried out in the Metallurgy Department of the Royal College of Science and Technology whilst the author was in receipt of a research grant from the Metallurgy Department Reserve Fund and latterly from the Union Carbide and Carbon Corporation.

The author wishes to express his gratitude to Dr. J. Taylor for his most valuable advice on both the experimental and theoretical problems which arose during the course of this work.

The author would also like to thank Professor E. C. Ellwood for the interest he has shown in this work.